CONF-9406335--1

John G. Merkle[1]

PATTERNS AND PERSPECTIVES IN APPLIED FRACTURE MECHANICS

Reference: Merkle, John G. **"Patterns and Perspectives in Applied Fracture Mechanics,"** Fracture Mechanics: 26th Volume, ASTM STP 1256, Walter G. Reuter, John H. Underwood, and James C. Newman, Jr., Eds., American Society for Testing and Materials, Philadelphia, 1995.

ABSTRACT: This fifth Jerry L. Swedlow Memorial Lecture begins with a brief philosophical and historical overview of applied fracture mechanics, particularly as it pertains to the safety of pressure vessels. It then progresses to a more-or-less chronological panorama of experimental and analytical results pertaining to the important subject of constraint, a fundamental aspect of fracture mechanics in which Jerry Swedlow had a keen interest and to which he made valuable contributions. To be truly useful and dependable in application to the safety analysis of real structures, new analysis developments must be physically realistic. That means that they must accurately describe physical cause and effect. Consequently, before useful mathematical modeling can begin, a pattern of cause and effect must be established from experimental data. This can be a difficult and time consuming process, but it is worth the effort. Accordingly, a central theme of this paper is that, consistent with the scientific method, the search for patterns is constant and vital. This theme is well illustrated historically by the development of small, single-specimen, fracture toughness testing techniques. It is also illustrated, at the end of the present paper, by the development, based on two different published large-strain, elastic-plastic, three-dimensional finite-element analyses, of a hypothesis concerning three-dimensional loss of constraint. Specifically, it appears that, at least in standard compact specimens, when a generalization of Irwin's thickness-normalized plastic-zone parameter, β, reaches a value close to 2π, the through-thickness contraction strain at the apex of the near-tip logarithmic-spiral slip-line region becomes the dominant negative strain accommodating crack opening. Because slip lines passing from the midplane to the stress-free side surfaces do not have to curve, once these slip lines are established, stresses near the crack tip are only elevated by strain hardening and constraint becomes significantly relaxed. This hypothesis, based on published three-dimensional elastic-plastic analyses, provides a potentially valuable means for gaining additional insight into constraint effects on fracture toughness by considering the roles played by the plastic strains as well as the stresses that develop near a crack tip.

Keywords: Fracture mechanics, pressure vessels, fracture toughness, small specimen testing, flawed structural components, thickness effects, constraint.

---

[1]Research Specialist, Oak Ridge National Laboratory, Oak Ridge, Tennessee 37831.

DISCLAIMER

It is an honor to be invited to present the Fifth Professor Jerry L. Swedlow Memorial Lecture. Jerry Swedlow set a personal example of insight and quality in research, as well as an example of professional service, that we can all admire. I've tried to prepare this paper with these two examples in mind. By fortunate circumstance, this paper develops a focus on one of the very subjects that attracted Jerry's keen interest as a graduate student and held it throughout his career, that of the effects of thickness on fracture toughness, or slightly more generally, the three-dimensional aspects of constraint. This paper begins with some overall philosophy about fracture mechanics. It then progresses to a brief historical overview of some of the important experimental and analytical developments in fracture mechanics, especially as they relate to pressure vessels. Next a more or less chronologically based chain of evidence about what have come to be called constraint effects on fracture toughness is developed. Finally, the paper concludes with some recent evidence, and a hypothesis, about three-dimensional loss of constraint, especially in standard compact specimens.

It is easy to be positive and enthusiastic about fracture mechanics because it is an important and challenging field for several good reasons. It deals with an important real problem, the imperfection of real structures. By means of fracture toughness, it does what stress analysis alone cannot do; it enables the quantification of safety margins against fracture for real, imperfect structures. It makes full use of material science, nondestructive examination, thermal analysis, stress analysis, and probabilistic information. Nothing is overlooked. Interdisciplinary teamwork is essential. An important aspect of the behavior of structural metals is that crack-tip yielding precedes fracture. Therefore, a basic understanding of elastic-plastic metal behavior is required. Furthermore, fracture toughness is a unique material property. Its value cannot be reliably synthesized from other material properties. It must be calculated from sharp-cracked specimen data. With respect to analysis methods, some relationships in fracture mechanics exist in algebraic closed form. Others can only be obtained numerically. A partnership between algebraically direct and iterative numerical analysis is required. Finally, development and application of fracture mechanics requires proper use of the scientific method. Experiments and analyses must be coupled. *The search for patterns is constant and vital.*

To establish a perspective on applied fracture mechanics as it now exists, a look at its history is helpful. Table 1 lists some historically key issues and developments in fracture mechanics, emphasizing those that have been particularly significant with regard to quantifying the safety margins of pressure vessels. There was a time when brittle fracture was described simply in terms of catastrophic failure without warning, due to what was believed to be the reaching of a cleavage stress before yielding, a condition caused by triaxial stress concentration. The realization that, in structural metals, macroscopic cracks are a necessary cause of brittle failure was the key to modern fracture mechanics. From that realization flowed the concepts of elastic strain energy release rate [1], G_I, and the linear-elastic stress-intensity factor [2], K_I, as well as their critical values. In some structural metals, loading rate and crack-front-motion induced strain-rate effects were observed and appropriate analyses were developed [3, 4]. Effects of specimen size, especially thickness, on fracture toughness were observed and provisions made to deal conservatively with these effects [5]. Pressure vessel steels were characterized, first in terms of their thick-section dynamic impact

TABLE 1--Some historically key issues and developments in fracture mechanics for pressure vessels

- Brittle fracture: catastrophic failure without warning (up to early 1950's).
- Basic material behavior; is that all there is to it (up to early 1950's)?
- The involvement of cracks (starting in late 1940's).
- Elastic strain energy release rate; G and G_{Ic} (1954).
- The elastic stress intensity factor; K_I and K_{Ic} (1957).
- Loading rate and strain rate effects (1960's).
- Effects of size, especially thickness, on toughness (1970's).
- Characterizing pressure vessel steels (1970's).
- Initial codes, standards and technical basis documents; ASTM E399, WRC-175, ASME Section III Appendix G (1970's).
- Measuring toughness with reasonably sized specimens (1970's).
- CTOD and the *J* Integral (1965 and 1970).
- Determining the behavior of cracked structural components (1970's).
- ASME Section XI Appendix A (1974).
- Size and geometry effects (1980's).
- Ductile crack growth (1980's).
- E561, E813, E1152, E1221, and E1290 (1980's).
- ASME Section XI appendices for piping (1990's).
- Computers come of age (1990's).
- Constraint (1990's).
- Shallow cracks (1990's).
- Ductile hole growth and cleavage initiation sites (1990's).
- Statistical variability of cleavage toughness (1990's).

energy [6] and then in terms of their static [7], dynamic [8] and crack arrest [9] fracture toughness values. Initial versions of American Society of Mechanical Engineers (ASME) codes, American Society for Testing and Materials (ASTM) standards, and Welding Research Council (WRC) technical basis documents were written and published, as mentioned in Table 1. It soon became apparent that developing the experimental and analytical methods for measuring fracture toughness with reasonably sized specimens was going to be a major long-term challenge. The crack-tip-opening displacement (CTOD) and J-Integral parameters became prime candidates for this job. As single specimen J-Integral testing techniques were being developed, attention also became focused on determining the performance of cracked structural components, which display various unique behavioral characteristics of their own. Once linear-elastic fracture mechanics (LEFM) had reached a sufficient level of maturity, its essentials were incorporated into Appendix A of Section XI of the ASME Code [10], for the purpose of evaluating flaw indications discovered by nondestructive inspection. The J Integral was used to characterize ductile crack growth, and once again size and geometry effects became apparent [11]. Several more ASTM standards were completed and published, three relating to tearing resistance curves, one for crack arrest and one for CTOD testing. Appendices to the ASME Code were written to describe acceptable methods for performing ductile tearing instability analyses for flawed piping, as well as safety margin calculations for vessels containing materials with relatively low ductile tearing resistance. Then as computers and their software grew in capability, attention focused anew on the details of crack-tip deformation and stress distributions, creating the prospect of finally understanding the subject of constraint. Specimens with shallow cracks were tested and analyzed [12, 13] and the detailed modeling of ductile hole growth began in earnest [14]. Modeling the onset of unstable cleavage may not be far behind. The statistical variability of cleavage fracture toughness has already become a subject in its own right [15] despite the present lack of certainty concerning the exact sequence of events that leads to unstable cleavage.

Because fracture mechanics is a relatively new branch of knowledge within the field of structural engineering, opportunities for the development of new problem solutions and analysis procedures have abounded. However, to be truly useful and dependable in application to the safety analysis of real structures, these new problem solutions must be more than just mathematically or computationally ingenious. They must also be physically realistic. That means that they must accurately describe physical cause and effect. Consequently, before useful mathematical modeling can begin, a pattern of cause and effect must be established from experimental data. This can be a difficult and time consuming process, but it is worth the effort. Table 2 lists some of the analytical aspects of fracture mechanics that have been particularly dependent upon experimental data for their development. The remainder of this paper focuses on a selection of subjects from Table 2, particularly those related to size, geometry and rate effects on fracture toughness.

SMALL SPECIMEN TESTING

In the course of performing the static and dynamic fracture toughness testing of pressure vessel steels described in Refs. 7 and 8, some important fundamental facts about such testing soon became apparent. Because of the crack size dependence of all crack-tip stress

TABLE 2--Analytical aspects of fracture mechanics particularly dependent upon experimental data for their development

- Effects of yielding
  - Small specimen toughness testing
  - Cracks in structural members
  - Warm prestressing
- Constraint
- Stable ductile crack growth
  - Upper shelf
  - Before cleavage
- Strain rate effects, including crack arrest
- Effects of temperature and irradiation
- Effects of environment
- Fatigue
- Calculated versus measured strains and displacements
- Statistical effects of crack length
- Interactions between fracture and plastic collapse

intensity parameters, large specimens were required in order to obtain valid linear-elastic fracture toughness data. For lower and intermediate yield grade steels with adequate toughness for ensuring structural safety, statically loaded fracture toughness specimens of reasonable size will usually yield before fracturing. Therefore, the proper calculation of fracture toughness from laboratory tests of reasonably sized specimens requires inelastic analysis according to an analytically defined and physically meaningful fracture criterion. For practical purposes, laboratory specimens must be analyzable with single-specimen formulae. Such testing and analysis capabilities did not exist in 1970. Consequently, the search began for single-specimen test and analysis techniques applicable to small specimens that yield before fracturing, and results were soon forthcoming.

There were three candidate approaches for calculating fracture toughness from reasonably sized small specimens that yield before fracturing. These were (1) CTOD [16], (2) equivalent energy [17], and (3) the J Integral [18]. The CTOD was physically defined, in terms of single-specimen formulae, for the rigid-plastic behavior of laboratory specimens. However, analytical definitions for flaws in structures were lacking, except for definitions in terms of K_I and G_I that did not have the same analytical basis as the definition for laboratory specimens. Equivalent energy was an empirical concept with no exact physical definition in terms of crack-tip conditions. Although a single-specimen analytical definition existed in terms of global conditions for single load pairs, the definition could become ambiguous for distributed forces and thermal loads. The J Integral had strong potential advantages in terms of its physical meaning and analytical basis, but it was experimentally unproven and there were no single-specimen formulae available. Rice's derivation of the J Integral [19] had begun with an inquiry into the meaning of nonlinear work per unit crack extension area. It turned out that this energy rate was also the integral of work density with vertical distance progressing around the blunted crack-tip contour. Another integral over a connecting arbitrary internal path was formulated in terms of stress and strain to be equal to the blunted crack-tip integral, thus becoming an indirect measure of nonlinear crack-tip conditions. This was the J Integral.

Some key developments occurred at the Westinghouse Research Laboratory (WRL) in 1971. On April 13, 1971, a meeting of WRL staff and consultants took place* at which the general subject of elastic-plastic fracture mechanics was discussed. Topics included Rice's fundamental derivations related to the J Integral, some ongoing multispecimen measurements of work per unit crack surface area, i.e., J-Integral values, being made by Landes and Begley at WRL, and empirically successful applications of the equivalent energy method being made at the Oak Ridge National Laboratory (ORNL). In response to a presentation by Prof. H. T. Corten on ORNL's equivalent energy applications, Rice made an apparently extemporaneous commentary during which he developed the rigid-perfectly-plastic version of his now well known single-specimen J formula for a deeply cracked beam in pure bending.* Soon after the meeting at WRL, Landes and Begley presented their experimental demonstration of the J Integral as a fracture criterion at the 5th National Symposium on Fracture Mechanics (NSFM) [20, 21]. Later in the year, Rice improved his single-specimen beam formula to include strain hardening by adding the reasonable assumption that the net section bend angle depends only on the ratio of the applied moment to the fully plastic moment [22]. Rice's single-specimen beam and other formulae

---

* J. D. Landes, unpublished notes, April 13, 1971.

were presented the following year at the 6th NSFM [23]. Two other developments occurred soon after. Following Rice's lead, Merkle and Corten [24] applied the same class of assumptions to the compact specimen, which carries an axial force as well as bending, to produce a single-specimen J formula for the specimen most commonly used for measuring fracture toughness. Ernst, Paris, and Landes [25] then used the basic concepts of the deformation theory of plasticity to derive a method for adjusting calculated single-specimen J values for crack growth during loading, thus clearing the way for the measurement of J-R curves.

In the case of developing a soundly based method for measuring fracture toughness with reasonably sized small specimens, the pattern was fairly simple, namely, match previously measured valid data where it existed. The perspective, which was all important, involved applying basic principles and keeping all the criteria clearly in mind, namely that the chosen fracture toughness parameter must be (1) physically meaningful, (2) analytically defined, and (3) lead to single-specimen formulae.

CRACKS IN SPECIMENS REPRESENTING STRUCTURAL COMPONENTS

The emergence of the J Integral for measuring material fracture toughness with reasonably sized small specimens, loaded primarily in bending, did provide a satisfactory means of material characterization. However, it did not automatically lead to a sufficient degree of understanding of the behavior of flaws in structural test components, especially in the elastic-plastic range. Some load and geometry combinations tested showed toughness elevations above values obtained under conditions of high constraint. Some of the elevations were gradual, some were sudden. Other load and geometry combinations showed no toughness elevations. The effects of loading mode (tension versus bending; thermal loading), so-called constraint (longitudinal and transverse), and geometry (pressurized cylinders, nozzle corners, tensile bars, shallow cracks, through-cracks, and part-through cracks) remained to be better understood.

The effects of tension versus bending were revealed in a rather striking manner by a series of so-called gross strain tests performed by Randall [26], using long rectangular bars of A533, Grade B, Class 1 steel containing finite-length part-through surface cracks. Flaw tolerance was measured in terms of gross strain, defined as the ratio of axial displacement divided by gage length between two surface points on the centerline perpendicular to the crack plane. As shown in Fig. 1, the critical values of both the net section gross strain (ε_{gnc}) measured across the crack mouth and the gross section gross strain (ε_{ggc}) measured above or below the crack, for uniform tensile loading, underwent rapid increases with temperature between the yield strain and either the strain at the onset of strain hardening (~ 1-2%) or the tensile instability strain (~ 10%). The strain values above yield considerably exceed, and rise faster with temperature, than those calculated by LEFM, although the temperature at which the fracture strain equals the yield strain is roughly consistent with LEFM. By modifying the test fixture it was possible to load the gross strain specimens with a controlled combination of axial strain and bending strain, with the pattern of results [27] shown in Fig. 2. As positive bending strain increased relative to uniform tensile strain, the curve

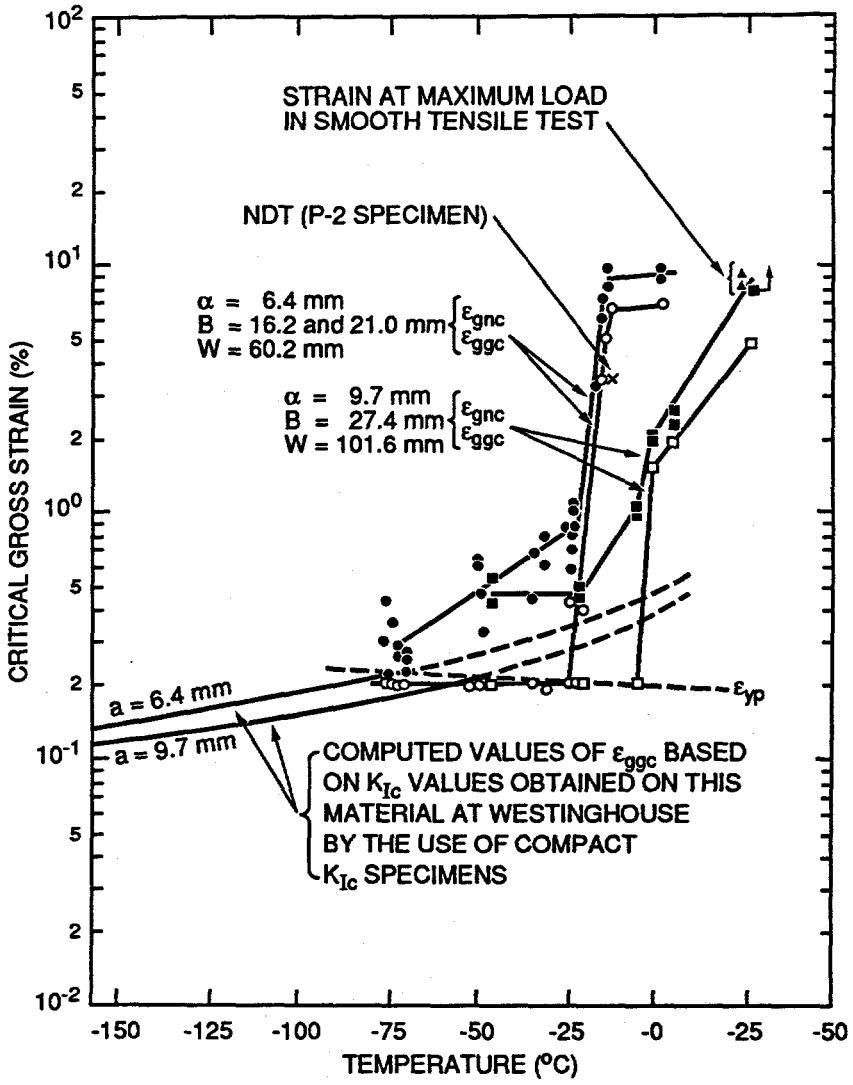

Fig. 1 Critical net and gross-section gross-strain curves for surface-cracked tensile specimens of A533 Grade B, Class 1, steel (from Ref. 26).

of front-face critical gross strain versus temperature decreased in average slope, appearing to approach the curve predicted by LEFM [28]. An apparently systematic effect of bending versus tension on elastic-plastic fracture toughness was experimentally demonstrated.

Following the gross strain tensile tests described in Ref. 26, considerably larger surface cracked tensile bars of the same material were tested at the Southwest Research Institute (SwRI) [29]. These specimens had cross sections 152 mm (6 in.) thick and 457 mm (18 in.) wide and contained fatigue sharpened finite-length part-through surface cracks between 57 mm (2.25 in.) and 111 mm (4.38 in.) deep. As shown in Fig. 3, the pattern of results, plotted here in terms of net section fracture stress versus temperature, was very similar to that for the gross strain tension specimens. The specimens fractured at a net section stress equal to the yield stress over a range of temperature, a

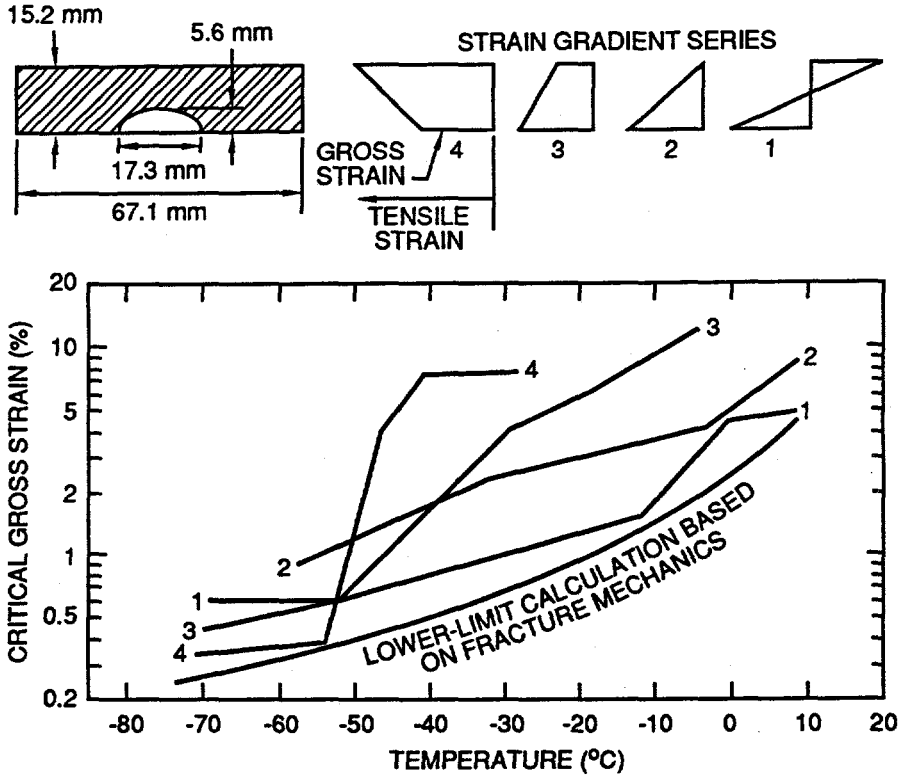

Fig. 2 Effect of strain gradient on critical gross strain curves for A533 Grade B, Class 1, steel (from Ref. 28).

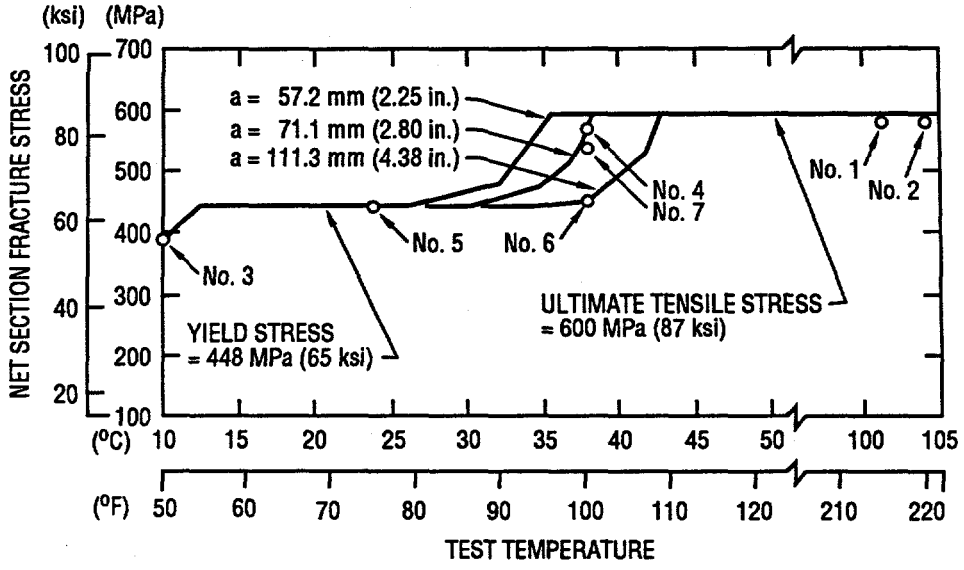

Fig. 3 Net-section fracture stress versus temperature curves for large surface-cracked tensile specimens of A533 Grade B, Class 1, steel tested at the Southwest Research Institute (from Ref. 28).

result qualitatively similar to that obtained two decades earlier in wide plate tests of World War II ship plate specimens [30]. Then, with further increase in temperature, the net section fracture stress rose steeply, with flaw size being a parameter, until it became equal to the ultimate tensile stress. The curves plotted in Fig. 3 were calculated by an approximate method of analysis that considered both yielding and a toughness elevation due to externally unrestrained net section transverse contraction [28]. Had the calculations been based on the plane-strain fracture toughness, they would have underestimated the fracture stresses.

At about the same time a series of geometrically similar drop-weight specimens of A516 and A533B steel, with thicknesses ranging between 9.53 mm (3/8 in.) and 203 mm (8 in.) were tested, both statically and dynamically, by the Martin Marietta Corporation in Denver, Colorado, to investigate thickness and flaw size effects on strain tolerance for flaws in bending [31]. Surface strains were measured with strain gages. In the elastic-plastic range, strain tolerances exceeded elastic predictions, leading to a general conclusion that yielding per se elevates fracture toughness [31, 32]. Although this general conclusion was soon contradicted, the Martin Marietta tests were in reality shallow-crack tests and their results are consistent with more recent similar tests.

Following the SwRI intermediate tensile tests and the Martin Marietta scaled drop weight tests, the Heavy Section Steel Technology (HSST) Program at ORNL performed a series of ten pressure tests to failure of 991 mm (39 in.) outside diameter, 152 mm (6 in.) thick, pressure vessels of A508 or A533B steel with external axial finite-length surface flaws, and two additional tests with axially oriented inside nozzle corner flaws [33]. The vessel diameter was chosen for practicality of fabrication and cost and the wall thickness was chosen to provide constraint conditions typical for full scale vessels [33]. A pair of test results from two vessels tested at room temperature is particularly illuminating with respect to the effects of structural geometry on effective fracture toughness for finite-length surface flaws. Vessel V-4, tested at 24°C (75°F) with a 76.2 mm (3.00 in.) deep, 210 mm (8.25 in.) long, axial surface flaw in an axial weld, failed at an outside hoop strain of 0.168%, close to the LEFM estimate. Vessel V-9, tested at 24°C (75°F) with a 30.5 mm (1.20 in.) deep inside nozzle corner surface crack, failed at an opposite inside nozzle corner strain of 8.4%, about ten times the LEFM estimate. It is apparent that the presence or absence of a transverse tensile stress in the plane of the crack (present for the axial flaw in the cylinder of vessel V-4 and absent, because of the two perpendicular free surfaces, at the inside nozzle corner of vessel V-9) exerted a strong influence on the effective fracture toughnesses. Other intermediate test vessels containing axially-oriented surface cracks in the vessel cylinders and tested at higher temperatures showed no pronounced toughness elevations above plane strain in the elastic-plastic range [34]. Thus the hypothesis that yielding per se elevates fracture toughness was not substantiated for relatively deep surface cracks subject to geometrically induced lateral tensile stress, but it was substantiated when such transverse tensile stresses were absent [28].

Following the intermediate pressure vessel tests, the HSST Program performed a series of thermal shock tests, using liquid nitrogen, on hollow cylinders of A508 steel of two different sizes, the larger of which were identical to the intermediate test vessel cylinders. These cylinders all contained shallow internal axially-oriented surface cracks, all but one of which were initially as long as the cylinders [35]. As shown in Fig. 4, none of these tests produced toughness values

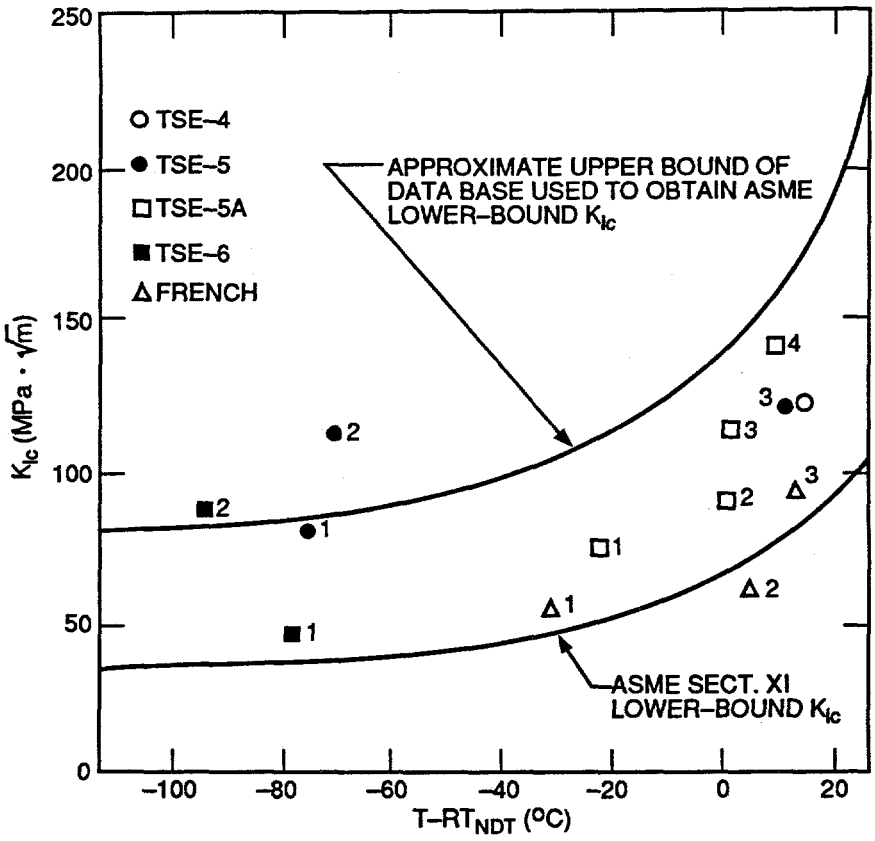

Fig. 4 Static-initiation fracture toughness data from French and ORNL thermal shock tests (from Ref. 35).

for their first or subsequent initiations that implied a consistent toughness elevation above the plane-strain scatter band [35]. Since elastically calculated thermal stresses at the inside and outside surfaces of a free-ended hollow cylinder are equal in the axial and circumferential directions, it is evident that transverse tensile stresses, as well as strain gradients, were once again playing a decisive role in maintaining constraint [36]. Similar results were obtained from subsequent tests of two intermediate test vessels containing shallow axially-oriented long surface cracks subject to pressurized-thermal-shock loading [37, 38].

Considering the small- and large-flawed structural simulation tests just described in their entirety, it is evident that a pattern involving a complex interaction of flaw size, geometry, loading mode, plane-strain fracture toughness and yield stress is emerging. However, this pattern is still incompletely understood, and it is not practical to expect that it can be made entirely clear by means of large structural simulation tests alone. Collectively, the effects described above have come to be called constraint effects and it is clear that these effects need to be studied, per se, analytically as well as experimentally.

INITIAL STUDIES OF CONSTRAINT

Studies of constraint effects actually did begin early in the development of fracture mechanics, as soon as it was recognized that

there were apparent size, geometry, and yield stress effects on measured values of fracture toughness. Irwin [39, 40] reasoned that the ratio of formally calculated plastic-zone radius to specimen thickness, for a through-cracked specimen, must be fundamentally related to crack-tip inelastic constraint effects. Over the course of several years, Irwin made several estimates of the relation between the ratio of plastic-zone radius to thickness and the degree of constraint, expressed in terms of fracture surface appearance and the characteristics of the fracture mode conversion from plane strain to plane stress. These estimates were phrased first in terms of the parameter α, where [39, 40]

$$\alpha = B/(K_{Ic}/\sigma_Y)^2, \tag{1}$$

B is specimen thickness, K_{Ic} is plane strain fracture toughness, and σ_Y is yield stress. Later the estimates were phrased in terms of the parameter β_c, where [41]

$$\beta_c = (K_c/\sigma_Y)^2/B \tag{2}$$

and K_c is the measured non-plane-strain value of fracture toughness. An empirical equation [41, 42],

$$\beta_c = \beta_{Ic}(1 + 1.4\ \beta_{Ic}^2), \tag{3}$$

in which

$$\beta_{Ic} = 1/\alpha, \tag{4}$$

was developed by Irwin for estimating values of K_{Ic} from measured values of K_c, or the reverse. Tables 3 and 4 show estimates made by Irwin of the significance of α and β_c values, in terms of fracture mode, including the references in this paper from which the individual estimates were obtained. It is clear that Irwin's estimates could only be semi-quantitative, but also that they were an important guide to the establishment of conservative criteria for plane-strain fracture toughness testing. Equation (3) was put to an early important application by Wessel [46], that of conservatively but realistically adjusting experimental data to estimate the plane-strain fracture toughness of a heat-treated ASTM A-372, Class 4, steel used for critical U.S. Navy air flasks. The successful outcome of this effort was a key factor in the acceptance of the discipline of fracture mechanics by the U.S. Navy.**

Recognizing that constraint effects on fracture toughness pertain to physical phenomena very close to a blunting crack tip, some investigators, including Lubahn [47] and Weiss [48], attempted to develop stress state dependent ductility relationships for use with elastic or elastic-plastic crack-tip stress analyses. Building on the results of a scaled-up, slow-bend, Charpy test performed by Lequear and Lubahn [49], which demonstrated essentially a plane strain condition at the notch root, Clausing [50] developed a procedure for estimating plane-strain ductility. Plane-strain ductility was measured directly by testing deep doubly-face-notched tensile bars and measuring the final

---

** E. T. Wessel, personal communication to J. G. Merkle, November 2, 1983.

TABLE 3--Estimated Significance of a in Terms of Fracture Mode.

$\alpha = 1/\beta_{Ic}$	Significance	Reference
0.2	Plane stress	39
0.25	Shear mode	39, 40
0.50	Beginning of transition to plane strain	42
0.67	80% shear	43
1.0	Plane strain; Mid-range of transition; Less than 50% shear	40 42 44
1.2	End of transition to plane strain	42
1.5	Beyond transition to plane strain	42
2.0	Plane strain; Possibly 50% shear	39 43
2.5	ASTM E399	

TABLE 4--Estimated significance of β_c in terms of fracture mode.

β_c	Significance	Reference
0.55	Less than 5% shear	41
1.9	Plane strain; Beginning of fracture mode transition to plane stress	41 42
2.7	45-60% shear	41
π	Near mid-range of fracture mode transition; Still less than 50% shear	41, 43 45
2π	Sometimes 70-80% shear; Sometimes nearly 100% shear	41 43, 44, 45

contraction of the remaining ligament after failure. For convenience in application, this strain was correlated empirically with the energy to maximum load in a slow-bend ordinary Charpy test. Attempts to relate plane-strain ductility to plane-strain fracture toughness were then made empirically by Barsom [51] and analytically by Merkle [52]. Merkle's approach dealt directly with the finite root radius of the physical crack, by using Malkin's and Tetelman's estimate [53] of an initial root radius value for A533B steel and calculating the applied notch root strain by integrating an incremental version of Neuber's equation [54] for notch-tip stresses and strains beyond yield. A resulting estimate of K_{Ic} for A533B steel [52] is shown in Fig. 5, which at least supports some optimism concerning the estimation of K_{Ic} values from Charpy data. Note that the results shown in Fig. 5 are an exception to the postulate

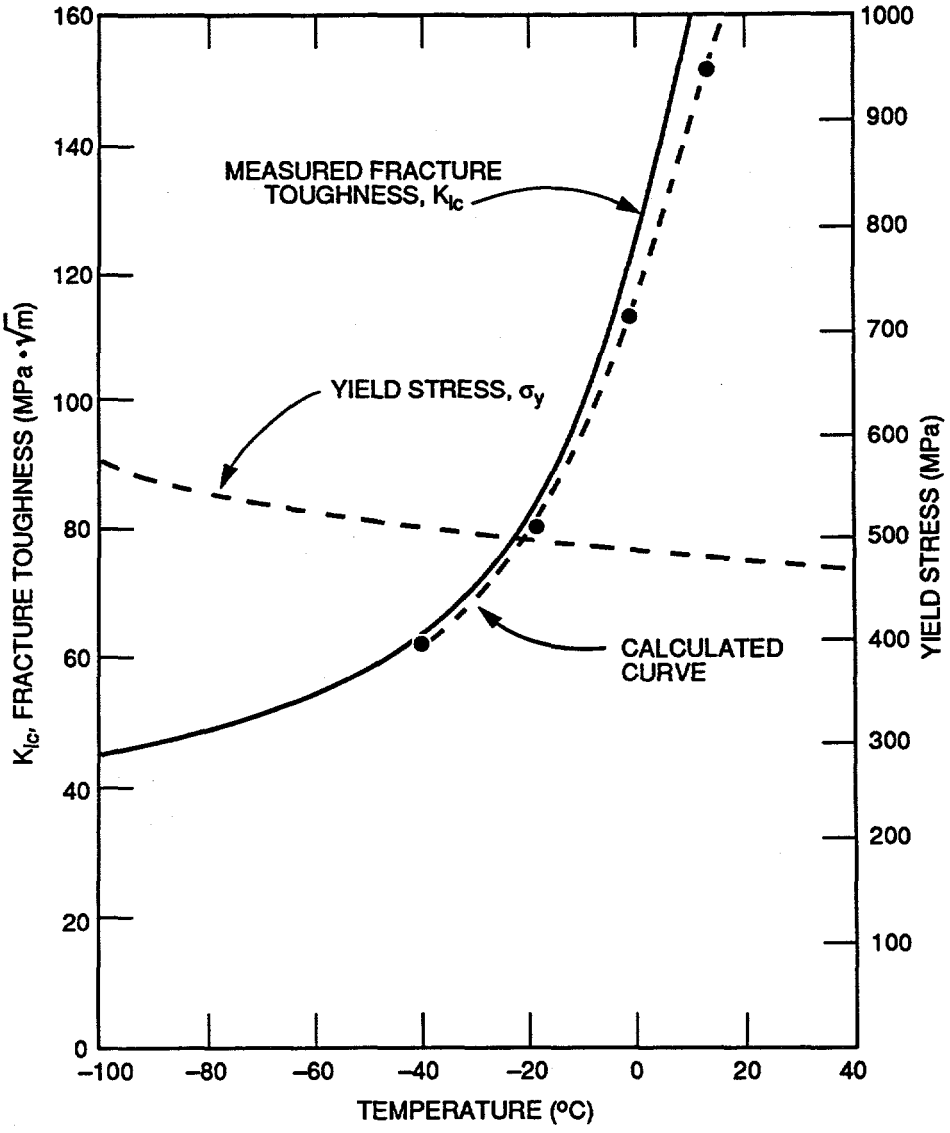

Fig. 5 Comparison of fracture toughness estimated from plane-strain ductility (plotted points and broken rising curve) with the curve based on valid large-specimen directly-measured data (solid curve) for A533 Grade B, Class 1, steel (from Ref. 52).

that determinations of fracture toughness require sharp-cracked specimens. However, the existence of several other useful correlations between Charpy data and fracture toughness also implies that the sharp-crack postulate might not be absolute.

In the course of applying the CTOD and J-Integral analysis methods to laboratory specimens, it was observed, both analytically and experimentally, that the relationship between the two fracture toughness parameters is subject to apparent constraint effects. Table 5 summarizes typical analytically and experimentally calculated values of the constraint parameter, m, in the alternate expressions

$$J = m\ \sigma_Y\ \delta \text{ or } J = m\ \sigma_f\ \delta, \tag{5}$$

where σ_Y and σ_f are the yield and flow stresses, respectively, and δ is the CTOD, demonstrating that as transverse constraint increases, the CTOD value corresponding to a given J value decreases [55-59]. The constraint parameter m is useful in estimating J from δ, or the reverse, for specified conditions, but it has not yet been developed into a means of predicting constraint effects on fracture toughness, per se.

Apparent constraint effects were also observed experimentally in the form of a specimen geometry effect on the magnitude of J - Δa ductile tearing resistance curves, where Δa is the amount of crack growth by ductile tearing. Landes, McCabe, and Ernst [60] observed that the J_M - Δa tearing resistance curve for a center-cracked tensile specimen of A533B steel was higher than the curve for other geometries. It was deduced that the reason for this difference is that slip lines can extend from the crack tips in a center-cracked tensile specimen to free specimen edges without curving, whereas in the other specimens they cannot do so. Since stress elevation at crack tips increases as the slip lines that intersect at the crack tip become more curved, it follows that the crack tips in the center-cracked tensile specimen are subject to less stress elevation due to yielding than in the other geometries. This is an important observation, and may have a significant bearing on transverse as well as longitudinal (in-plane) constraint effects.

Differences in crack-tip stress distributions under tensile and bending loads were also investigated analytically, using plane-strain, finite-strain, elastic-plastic finite-element analyses to reveal important details. McMeeking and Parks [61] observed that in bending, as J increases, the values of crack opening stress normalized by the flow stress, σ_{yy}/σ_o, remain almost exactly equal to their small-scale yielding values at equal values of normalized distance, $R/(J/\sigma_o)$, at least to $L\sigma_0/J = 42$, where L is the ligament dimension.. However, in tension, the normalized stresses immediately begin to decrease with increasing J, beyond the stress peak, which occurs at a value of $R/(J/\sigma_o)$ about equal to 1.0. These early near-crack-tip stress analyses served both to illustrate and define geometry effects on crack-tip stress distributions, but also to warn analysts that elastic-plastic near-crack-tip stress distributions must be functions of more than one parameter. This warning did not go unheeded.

Early in the development of fracture toughness testing, shallow cracks were avoided, because they were likely to lead to specimen yielding and higher values of fracture toughness than would otherwise be measured with deeply cracked specimens. However, as experience in CTOD testing accumulated, deliberate testing of shallow cracked specimens in bending commenced in order to realistically simulate certain structural

TABLE 5--Values of the constraint parameter m in the relation between J and CTOD, $J = m\ (\sigma_Y \text{ or } \sigma_f)\ \delta$.

Investigator	Ref.	Year	Reference Stress	Plane Stress	3D	Plane Strain	Remarks
Harrison	55	1975	σ_Y	1.3		1.7	
Dawes	56	1977	σ_Y		1.5-2.1		Experimental
Wellman, Rolfe, & Dodds	57	1984	σ_Y	1.0		2.0	
			σ_f	1.2		1.6	
Wilson & Donald	58	1989	σ_Y		1.73		Experimental
Sorem, Dodds, & Rolfe	59	1990	σ_f		1.4 1.6 1.7		Shallow; E-PP Shallow; A-36 Deep; A-36

safety situations [56, 12]. Eventually, such data were also interpreted in terms of numerical calculations of J [59, 13]. Sorem, Dodds, and Rolfe [62] showed conclusively that the shallow-crack toughness elevation in bending is caused by slip lines from the crack tip curving backwards to reach the front-face free surface, which they do not do in a deeply cracked specimen. The detailed effects of such a plastic zone development, in terms of the near-crack-tip stresses, were investigated later by others.

With the aforementioned experimental and analytical information in hand, plus the vast improvements in computing technology that have taken place in recent years, analysts were in a position to economically investigate the details of crack-tip stress distributions, at least in two dimensions, in order to formulate and test hypotheses concerning constraint. Since the analyses of Ref. 61 had illustrated the non-uniqueness of elastic-plastic crack-tip stress distributions with respect to J alone, attention focused on the identification of a practical second parameter. The first candidate was a parameter already routinely calculated from photoelastic data [63], namely the elastically calculated nonsingular horizontal normal stress near the crack tip, σ^{o}_{nn}. In fracture mechanics constraint investigations [64, 65], this stress became known as T_{11}, or more commonly, simply the T stress. Elastic-plastic, large strain, so-called modified boundary layer analyses of circular regions containing crack tips and subject to the elastic boundary tractions or displacements corresponding to K_I and T show that positive values of T raise the near-crack-tip stresses only slightly, while negative T values lower them appreciably [64, 65]. Although predictions of near-crack-tip stresses based on the T stress still seem useful near limit load [65], other investigators [66] have chosen to focus on another second parameter, the definition of which is based on the stresses that develop within a few multiples of the CTOD from the blunting crack tip. This is known as the Q parameter, which represents what in two dimensional analysis turns out to be an approximately constant hydrostatic stress difference in the forward sector, equal to $Q\sigma_o$, between the near tip normal stresses beyond the stress peak and the values which exist under small-scale yielding conditions at the same normalized distance from the crack tip [66]. Figure 6 illustrates the variations of normalized hydrostatic stress on the plane of crack extension with normalized distance, obtained from plane-strain, large-strain, modified-boundary-layer analyses using K_I and T to determine boundary conditions, as presented in Ref. 66. Beyond the stress peak, the curves become virtually parallel, thus supporting the Q parameter concept. The curves in Fig. 6 are therefore labeled with the calculated values of Q. These results show that for two-dimensional analyses, a two parameter characterization closely represents elastic-plastic near-crack-tip stress distributions beyond the stress peak. However, for a given geometry and loading condition, the relation between J and Q is not known in advance, but must be determined numerically. The rising stress distribution between the blunted crack tip and the stress peak is quite insensitive to T and Q, because constraint conditions in this large-strain region are dominated by proximity to the stress-free surface of the blunted crack tip. At least within the limits of a one parameter characterization based on CTOD, this same segment of the normalized stress distribution is also relatively insensitive to uniform variations in the transverse strain [67]. The range of the rising stress distribution, and therefore the magnitude of the stress peak, does depend on constraint, through its effect on the falling stress distribution beyond the stress peak. In particular, a decrease in

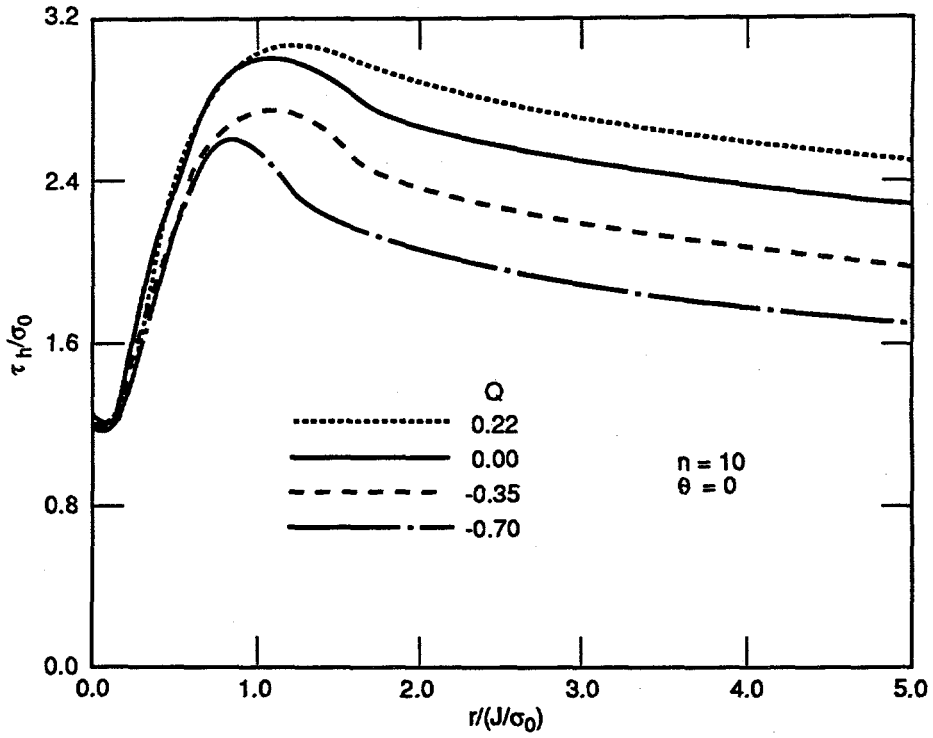

Fig. 6 Effect of variations in the T stress applied to a modified-boundary-layer model, on the near-crack-tip normalized hydrostatic stress, expressed in terms of the Q parameter (from Ref. 66).

constraint lowers the falling stress distribution, thereby lowering the stress peak.

Considering the approximate invariance of Q with the crack-tip polar coordinates r and θ in the forward sector, and the null effect of hydrostatic stress on yielding, it is understandable that Anderson and Dodds [68-70] could observe, in two-dimensional, elastic-plastic, small-strain, analyses, that normalized principal stress contours ahead of crack tips in finite bodies, within a range of stress values, tend to remain geometrically similar, although they usually decrease in size as yielding progresses. An example of these observations, for a shallow crack in a beam [70], is shown in Fig. 7. On this basis, Anderson and Dodds [68, 69] proposed to use the absolute area enclosed within an arbitrarily chosen principal stress contour as a fracture criterion. Because of the observed geometric similitude of principal stress contours, the resulting fracture estimates are independent of the chosen stress value, as long as it is within the range of similitude. The method of application of this hypothesis is to construct a curve relating the small-scale-yielding values of J_{ssy} and the finite body values of J_{FB} that produce equal areas enclosed by the chosen principal-stress contour. Then, measured small-specimen values of J_{FB} at fracture can be adjusted to the corresponding large-specimen small-scale-yielding values on the basis of equal areas, or the reverse.

Although the normal stresses in the small-strain region of the plastic zone beyond a crack tip in finite bodies at low loads may be describable in terms of J and a hydrostatic stress difference coefficient Q, with respect to a reference small-scale-yielding (SSY)

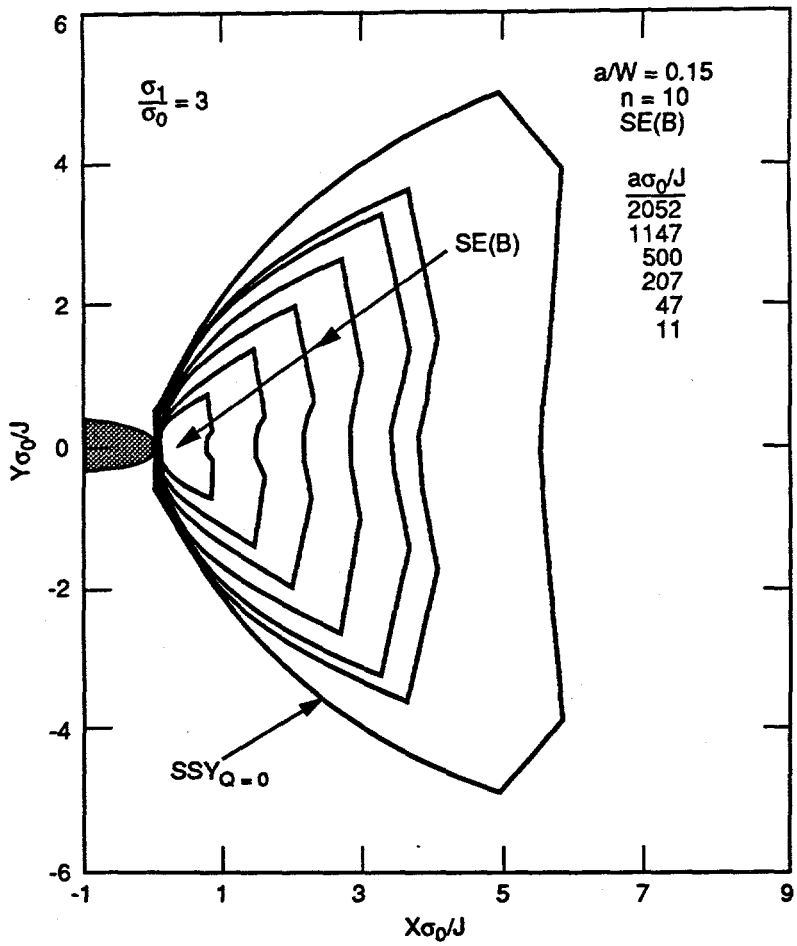

Fig. 7 Normalized principal stress contours for a succession of normalized increasing J values (from Ref. 70).

solution, this does not always remain true at higher loads. At higher loads, significant differences in terms of the shear stresses, and therefore also the plastic strains, sometimes appear with respect to the reference SSY solution [71, 72]. These differences cannot be reconciled by means of a hydrostatic stress change, because hydrostatic stress changes have no effect on yielding, and therefore no effect on the shear stresses and the plastic strains [71, 72]. For this reason, mathematical investigations, at present based on small-strain theory, have recently been undertaken to obtain additional terms in the elastic, power-law strain-hardening, series expansions for which the HRR solution is the set of initial terms [71-76]. Good results have been obtained by means of a three-term, variables-separable, series expansion for all the stresses, strains and displacements near a crack tip in a material with a Ramberg-Osgood stress-strain curve [73]. It turns out that the first three terms are often sufficient to match numerically calculated values of stress at all angles over most if not all of the plastic zone, for deep and shallow cracks and for low to high strain hardening exponents in both plane stress and plane strain [73]. In each case, the first term in the series represents the HRR solution [74, 77-79]. In the case of Mode I, for plane stress, all three stress terms are controlled by J alone, while for plane strain the second and third terms are controlled

by a single independent dimensionless coefficient, termed A_2 [71, 75], which can be numerically calculated by either point matching or least-squares fitting to finite-element data [71-74]. One reason for the sufficiency of a three-term stress series is the empirical observation that, based on the separability of the variables r and θ in each term, the functions of θ in the third and higher order terms are almost proportional at all values of θ, thus allowing, by close approximation, a collection of the third and higher order terms into a single term [73]. In addition, the fourth and higher order stress terms are apparently relatively small in magnitude compared to the third term so that the numerical determination of A_2, which also appears in the second term, is not rendered inaccurate. For small-scale yielding, as modeled by the modified boundary layer (MBL) method, numerically calculated differences in shear and effective stresses in the forward sector between the HRR and the complete solutions are small compared to those for the normal stresses [73, 76]. This implies that normal stress differences are due to a hydrostatic stress, which therefore justifies the J-Q approach for relatively low loads. However, for finite geometries under large-scale yielding, which is typical of laboratory test specimens in the transition range, shear and effective stress differences, and therefore plastic strain differences, can become significant [73]. Such differences cannot be corrected by the J-Q approach, but they generally can be and are well corrected by the J-A_2 approach. Although it is presently still necessary to employ full-field numerical analyses to determine the parameter A_2, in the absence of a single-specimen experimental method, the J-A_2 method does offer an improved mathematically rational method for describing the stress fields in the plastic zones extending from crack tips. Therefore, the parameter A_2 is a good candidate for a constraint parameter for stress-controlled fracture [74]. Similar comparative calculations in terms of strains, displacements, and transverse loading, are feasible but have not yet been published [72, 74]. In addition, the present theory is based on small-strain-theory and the assumption of an infinitely sharp initial crack, so the full extent of crack-tip blunting is not considered. With these limitations in mind, it does appear that higher order term analyses have the potential to be quite helpful in developing improved engineering fracture criteria in terms of either stress or strain [72, 74].

The foregoing examples demonstrate that analysis aspects of constraint for stationary cracks under plane-strain conditions have been greatly clarified by recent computational studies. However, other important aspects of constraint remain to be equally well understood. These include thickness effects, biaxial nominal-stress effects, effects of ductile crack growth prior to cleavage, crack-front-motion induced strain-rate effects and microstructural effects.

PRELIMINARY THICKNESS, BIAXIAL, CRACK-GROWTH AND METALLURGICAL ASPECTS OF CONSTRAINT

Although the recent two-dimensional plane-strain analytical treatments of constraint have certainly revealed the importance of in-plane (longitudinal) constraint effects, especially for shallow flaws, they have not proven that through-thickness (transverse) constraint effects are unimportant. Returning to basic physical reasoning and experimental observations, the fact that the side surfaces of standard through-cracked specimens are free of stress, and the observation of transverse contraction dimples at the crack ends, which grow with

increasing load, strongly imply a loss of stress triaxiality progressing through the thickness from the free surfaces toward the mid-plane with increasing load. Historically, thickness contraction effects were believed to be the main reason that measured fracture toughness values were observed to decrease with increasing specimen thickness, approaching an asymptote which implicitly corresponds to fracture initiation near the mid-plane before significant through-thickness stress reduction has occurred. Such reasoning was the basis for the thickness criterion chosen by ASTM for measuring linear-elastic-fracture toughness [5]. It also served as the qualitative definition of what was considered to be perhaps the most basic unsolved problem in fracture mechanics, that of transverse constraint. Because of its fundamental importance, the thickness effect on fracture toughness attracted Jerry Swedlow's attention and it was the subject of his Ph.D. thesis [80]. Using Irwin's data for 7075-T6 aluminum as an illustration, as shown in Fig. 8, Jerry attempted to formulate the three-dimensional elastic equations for a through-crack in a wide plate, finding that if the near-crack-tip stresses are expressed as products of functions of radius and angle, the transverse stresses would not be singular. This somewhat suspicious and physically unlikely result led to the decision to approach the elastic-plastic problem numerically. Jerry used the finite-element method to solve the plane-stress problem as a first step in understanding free-surface-induced transverse constraint effects. Although not a three-dimensional solution, Jerry's work was an early milestone in computational fracture mechanics.

One preliminary approach to a three-dimensional analysis is a two-dimensional generalized-plane-strain analysis. Such results, obtained

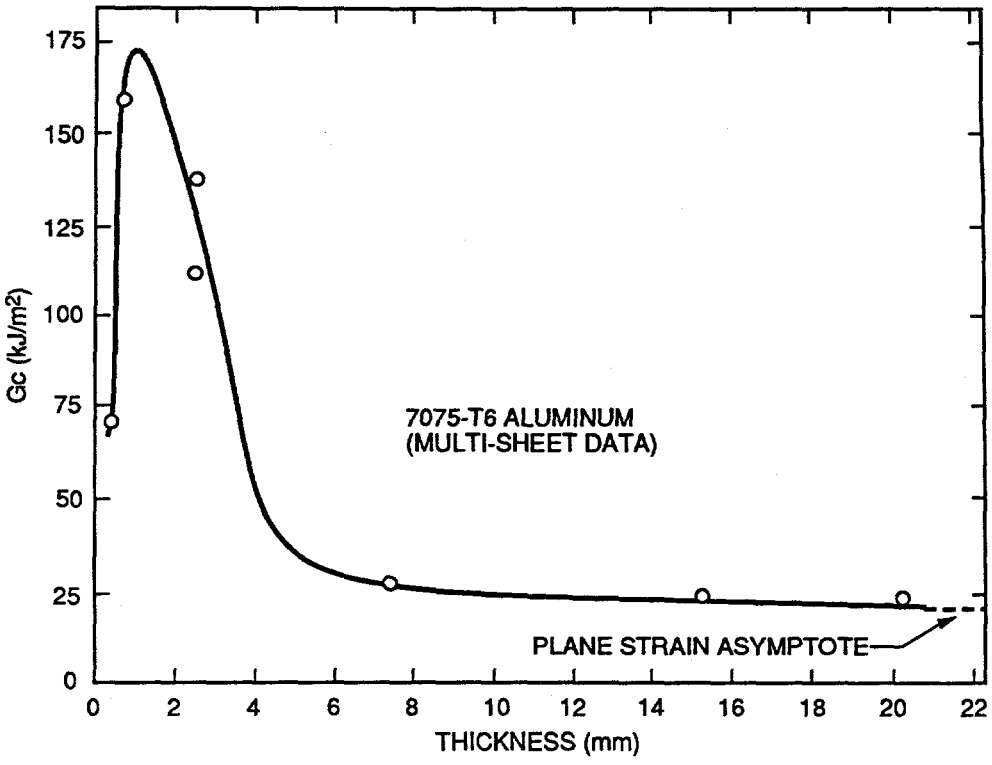

Fig. 8 Variation of critical strain energy release rate values with specimen thickness for 7075-T6 aluminum (from Ref. 80).

by Shum, for an elastic-plastic, large-strain analysis of a single-edge-notched tension specimen with a/W = 0.25, as shown in Fig. 9, show that under nominally LEFM valid conditions, positive variations in transverse strain at a given load have no significant effect on near-crack-tip stresses [81], for $r/(J/\sigma_0) \leq 2.5$. Although results were not presented in Ref. 81 for negative transverse strains, the results presented imply that thickness effects, when they do appear, may be due to phenomena that cannot be well modeled by a two-dimensional analysis. Further experimental and analytical investigations of biaxial-loading effects on the fracture toughness of reactor pressure vessel steels are in progress at ORNL [82]. However, three-dimensional analysis results are not yet sufficient to clearly define the important details of multiaxial stress and strain behavior near crack tips for biaxial loading [82].

The general observation that size effects on dynamic-initiation and crack-arrest fracture toughness are minimal, compared to those on static-initiation fracture toughness, is generally attributed to strain-rate effects on the yield stress. However, the observation made by Milne and Curvey [83] in 1982, as shown in Fig. 10, that stable ductile crack growth prior to cleavage initiation causes a progressive reduction and eventual elimination of size effects on the cleavage fracture toughness implies that something other than general strain rate effects may also be involved in this process. An analytical explanation for this phenomenon was recently developed by Varias and Shih [84] who, using a modified-boundary-layer, small-strain, elastic-plastic finite-element analysis, and equations appropriate for steady-state rate and inertia-independent crack growth, found that a high-constraint

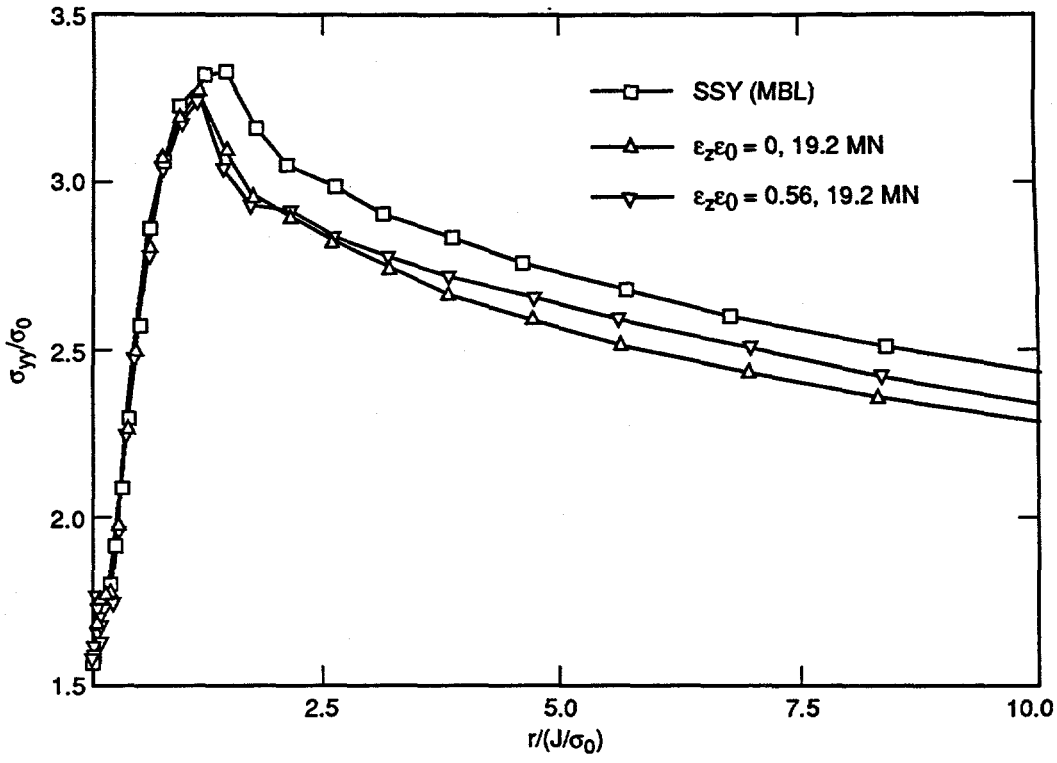

Fig. 9 Comparison of normalized near-crack-tip stresses for two generalized-plane-strain values from full-field analyses of a single-edge-notch specimen with a small-scale-yielding modified-boundary-layer solution (from Ref. 81).

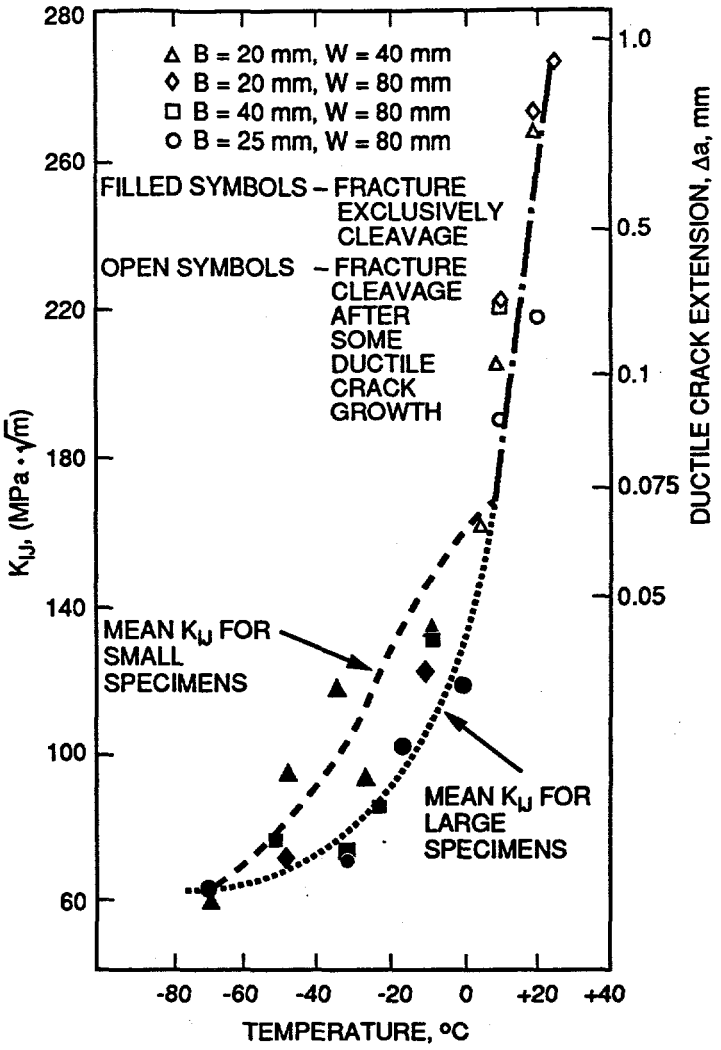

Fig. 10 Illustration of the convergence of small and large-specimen fracture toughness curves in the upper transition region, caused by constraint recovery due to ductile crack growth prior to cleavage (from Ref. 83).

single-parameter stress field always tends to develop during ductile crack growth, regardless of the level of constraint before crack growth. Tang and Dodds [85] confirmed the results of Ref. 84 by analyzing the early transient phase of crack growth. They found a progressive increase of the normal stresses in the region surrounding the crack tip, toward values generally slightly higher than the small-scale-yielding values. In the yielded region behind the growing crack, the horizontal stress was especially increased, apparently because of the resistance to the plastic contraction required to accommodate crack opening. This stress increase could be responsible for the elevation of the hydrostatic stress ahead of the crack tip and the observed reduced opening (so-called crack sharpening) characteristic of growing cracks.

Metallurgical studies have also shown that the effects of moving separations within and between individual grains are also extremely and fundamentally important in the development of unstable cleavage fractures. Averbach [86, 87] and Hahn [88], among others, have

elucidated the requirement for plastic strain in the single digit percent range to form a cleavage microcrack, and the immediate temperature and time-dependent competition that ensues between grain yielding, microcrack blunting and arrest versus continued cleavage propagation through successive grains. More recent research at the University of Maryland [89, 90] has led to the hypothesis that cleavage in reactor pressure vessel steels and welds occurs only when small rapidly moving ductile separations, which develop in vulnerable regions, cause the impingement of very high local strain rates on neighboring ferrite grains. A typical vulnerable region in base material is a local concentration of micron-sized carbide particles which can rapidly debond from the surrounding ferrite. In low-carbon weld metals, broken or debonding silicate particles play the same role [90]. Constraint can become involved in this process via the fact that elastically-releasable strain energy is the only available means of propagating cleavage microcracks, and this quantity depends strongly on the maximum principal tensile stress normal to the plane of the microcrack. In turn, the maximum principal tensile stress is elevated by an increase in the hydrostatic stress. Thus the relevance of stress triaxiality.

ADDITIONAL AXISYMMETRIC AND THREE-DIMENSIONAL CONSTRAINT ANALYSIS RESULTS

Although the assumption of plane strain has often been used for crack-tip stress analysis problems, either because it was believed to represent an actual physical limit approaching the crack tip or simply because it was a computationally expedient and reasonable two-dimensional approximation, not all important facts about constraint are revealed by such analyses. Jerry Swedlow realized this and consequently sought to perform some accurate crack-tip stress analyses involving no arbitrary assumptions about the transverse strain and its effects. Having observed first hand the difficulty of performing numerical three-dimensional elastic-plastic analyses, Jerry decided to take the intermediate step of studying a class of axisymmetric elastic problems. Swedlow and Ritter [91] performed elastic finite-element stress analyses of axially loaded thick-walled hollow cylinders containing either complete (360°) internal or external circumferential surface cracks. They defined positive crack front curvature for an internal surface crack as the ratio of the cylinder thickness to the crack-tip radius, and negative curvature for an external surface crack as the negative of the same ratio. The circumferential strain tangential to the crack front was always negative for an internal surface crack. While it was still negative for shallow external surface cracks it became positive for deeper external surface cracks. Thus it was numerically demonstrated that crack tips do not automatically create plane strain, and that the transverse strain at a crack tip for a given load type depends on specimen and flaw geometry.

As computing capabilities improved, innovations continued in the development and application of computational and analytical techniques to fracture analysis problems. Using the method of lines, Malik and Fu [92] succeeded in analyzing the problem posed by Swedlow in his thesis, the through-crack is a finite-thickness elastic-plastic plate. Elastic K_I calibrations and elastic-plastic crack-tip plastic zone contours and opening-mode strains approaching the crack tip were calculated and plotted as functions of load and thickness positions. These results demonstrated that three-dimensional elastic-plastic fracture analyses were becoming practical. Other available three-dimensional elastic crack-tip stress analysis results for various geometries were examined [93] and it was found that they all imply non-singular non-zero values

of strain tangent to the crack front. These transverse strains were negative for all cases examined, except for the deeply externally notched round tensile specimen, in qualitative agreement with the Swedlow and Ritter [91] results.

A recent series of three-dimensional, small-strain, elastic-ideally plastic finite-element analyses of through-cracked tensile and bending specimens shows vividly the effects of finite thickness that are not portended by two-dimensional analysis results. Newman et al. [94], calculated average constraint factors, α_g, defined as the ratio of the average opening-mode stress on the plane of crack extension within the crack-tip plastic zone, divided by the yield stress. As shown in Fig. 11, values of α_g, plotted versus $K/(\sigma_o\sqrt{w})$, where w is specimen width, tend to fall within the same range as the values of m in Eq. (5), the relation between J and CTOD. Furthermore, partly because they represent through-thickness averages, the curves representing combined transverse and longitudinal constraint effects, as determined by three-dimensional analyses, are noticeably different from, and lower than, those representing longitudinal constraint effects only, as determined by two-dimensional analyses. In contrast to the plane-strain results of Refs. 84 and 85, it was also found that the normal stresses near the crack tip in a through-cracked thin sheet are not greatly affected by crack growth [94]. This could be due to the fact that the transverse contraction strains accommodating crack opening are occurring primarily in the through-thickness direction, which is associated with a plane-stress boundary condition rather than an increasing value of σ_{xx} behind the crack tip. The stationary crack results in Ref. 94 agree qualitatively with other recent results, expressed in terms of J and Q, obtained by Shum [95] from two and three-dimensional elastic-plastic analyses of compact specimens. Consequently, it is clear that the estimation of constraint effects is best accomplished with three-dimensional analyses.

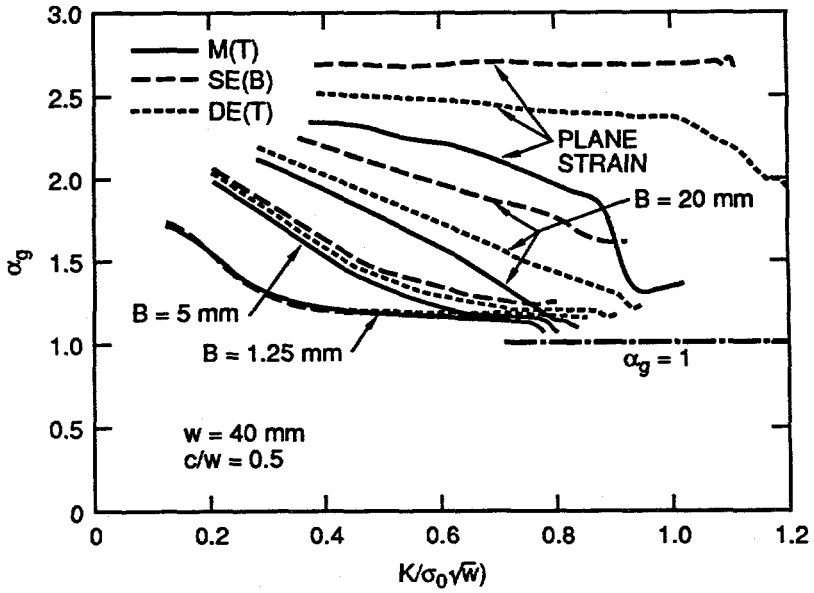

Fig. 11 Curves of α_g, the average normalized crack-opening stress on the plane of crack extension, within the plastic zone, from two- and three-dimensional elastic-ideally-plastic analyses (from Ref. 94).

Two recently obtained sets of two and three-dimensional large-strain, elastic-plastic finite-element analysis results for compact (CT) and other specimen geometries shed considerable light on the details of three-dimensional constraint effects, especially when the two sets of results are considered together. Figure 12 shows two and three-dimensional analysis results obtained by Brocks and presented by Sommer and Aurich [96], for double-edge-cracked tensile, center-cracked-tensile and compact specimens. Based on a reference cited [97], the Ramberg-Osgood stress-strain parameters for Brocks' analyses were σ_0 = 440 MPa, n = 7.7 and α = 1.0. In Fig. 12(a), the lower curve of each pair, for a given specimen geometry, is for J = 12 N/mm and the higher is for

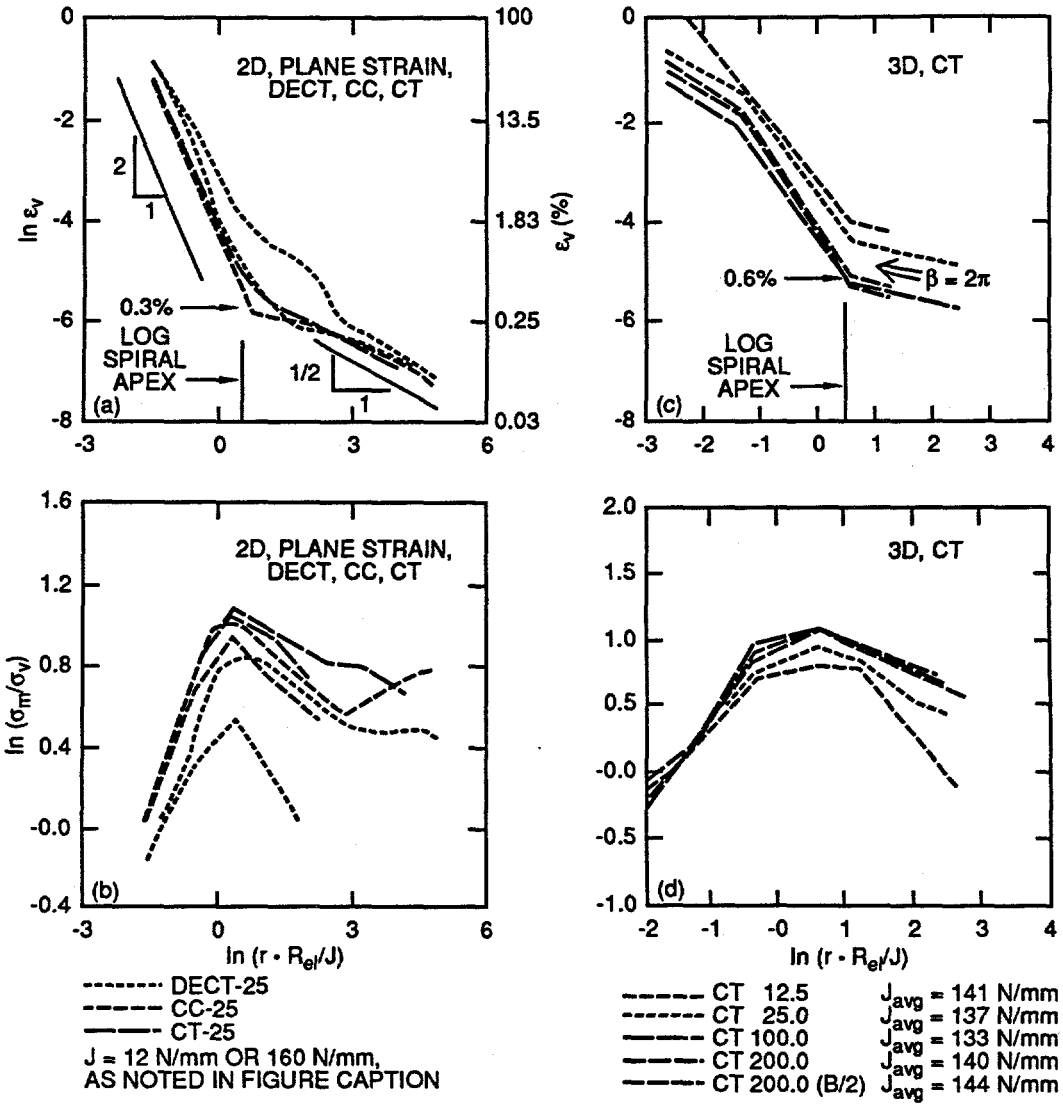

Fig. 12 Logarithmic plots of normalized near-crack-tip strain and stress for two- and three-dimensional large-strain elastic-plastic analyses of double-edge-cracked tensile, center-cracked tensile and compact specimens (from Ref. 96) In (a), the lower curve of each pair, for a given specimen geometry, is for J = 12 N/mm and the higher is for J = 160 N/mm. In (b), the reverse is true [97].

J = 160 N/mm. In Fig. 12(b), the reverse is true [97]. Figure 12(a) shows a log-log plot from two-dimensional plane-strain analyses of equivalent plastic strain versus normalized distance from the crack tip. In these coordinates, the strain curves are quite bilinear, with an abrupt change in slope at a logarithmic normalized distance of about 0.5. Assuming a value of m = 1.5 in Eq. (5) implies that the knee of the strain curves in Fig. 12(a) occurs at about r = 2.47 δ, which is close to the tip of the large-strain logarithmic-spiral slip-line zone [52]. The location of the stress peaks in Fig. 12(b) basically coincides with the knee of the strain plots. The slopes of the strain plots in Fig. 12(a) are nearly -1/2 beyond the knees of the curves, implying that deformations beyond the log-spiral region are still controlled by compatibility with the surrounding elastic material. Within the logarithmic-spiral slip-line region, the strain curves have slopes of about -2, in agreement with the small-plastic-strain solution for a yielded hollow cylinder, which is also characterized by logarithmic-spiral slip lines [52]. In the case of the three-dimensional results for the CT specimens, the strain plots in Fig. 12(c) are still piecewise linear, although they tend to be somewhat trilinear. The slopes of the segments meeting at the apex of the log spiral slip line region are not exactly -1/2 and -2, but they are reasonably close.

In the further examination of the same results, it is useful to employ a logical generalization of Irwin's definition of the β parameter in order to apply it to conditions beyond small-scale-yielding. Using the conversion

$$K^2 = EJ, \tag{6}$$

where differences between plane stress and plane strain are set aside for simplicity, Eq. (2) becomes

$$\beta = \frac{EJ}{\sigma_Y{}^2 B}. \tag{7}$$

In Eq. (7), the subscripts have been dropped in order to represent applied rather than critical values. The physical significance of Eq. (7) can be made clear by employing Eq. (5), which leads to

$$\beta = \frac{m}{\epsilon_Y}\left(\frac{\delta}{B}\right), \tag{8}$$

a relationship which has an easily understood meaning at all levels of loading. With these definitions it is possible to extend Eq. (3) beyond the limits of small-scale-yielding if experimental data substantiate the extension [98]. For Brocks' analysis, using a yield stress of 440 MPa (63.8 ksi), an elastic modulus of 207 GPa (30 x (10^6 psi) and ν = 0.3, it is possible to calculated the β values for each of the strain curves in Fig. 12(c). The strain curves rise as β increases, but only slightly until $\beta > 2\pi$ and then they rise noticeably more. The stress curves in Fig. 12(d) fall as the corresponding strain curves in Fig. 12(c) rise, and to the same relative degree, implying that $\beta > 2\pi$ does empirically correspond to the onset of a significant loss of three-dimensional constraint, as indicated by the "nearly 100% shear" note in Table 4. Until $\beta > 2\pi$, the equivalent plastic strain at the apex of the log-spiral slip-line region is about 0.6%. Afterwards it becomes significantly larger. These observations lend direct analytical support to those of McCabe [99], which were based on statistical analyses of

fracture toughness data in the transition temperature region, and which also independently imply that β reaching a value close to 2π constitutes a loss of constraint criterion.

The second set of results to be considered here are those obtained by Keeney [81] for the calculated values of transverse displacements close to the crack tip in a 1T-CT specimen, for which the yield stress at -75°C was assumed to be 483 MPa (70 ksi) and the elastic modulus 207 GPa (30×10^6 psi). Transverse displacement distributions were calculated for three different loads ranging beyond small-scale yielding, 29, 35, and 50 kN (6.5, 7.9, and 11.2 kips). Fig. 13 shows the plot of transverse displacement versus distance through the thickness for the load of 50 kN (11.2 kips). Notice in Fig. 13 that the curves for three different distances from the crack tip basically coincide, implying a condition of generalized-plane-strain close to the crack tip. Since

$$\varepsilon_z = \frac{\partial w}{\partial z}, \tag{9}$$

the negative slopes of the transverse displacement curves at z = 0 give the mid-plane transverse contraction strains. The calculated values of J, ε_z and β for the three loads are listed in Table 6, from which it can be seen that to a first approximation,

$$\varepsilon_z\ (\%) = -\ \beta / 10. \tag{10}$$

Referring to Fig. 12(c), it appears that when β becomes equal to 2π, the transverse contraction strain has become approximately equal to the equivalent plastic strain at the apex of the log-spiral slip-line region. Beyond this value of β, all of the transverse contraction strain needed to accommodate positive crack-opening strain near the

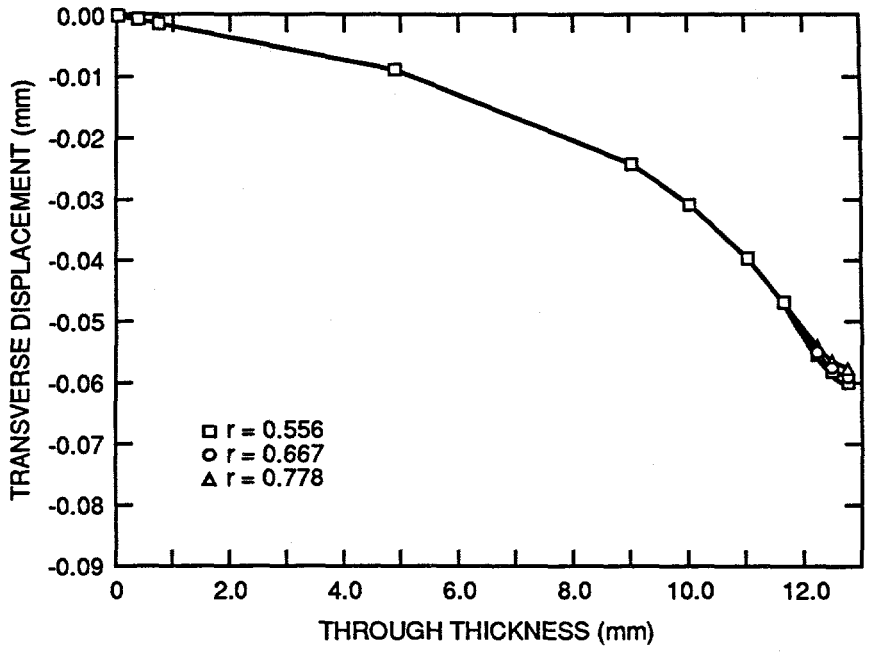

Fig. 13 Calculated near-crack-tip transverse contraction displacements in a compact specimen at three different distances from the crack tip (from Ref. 81).

TABLE 6--Three-dimensional elastic-plastic analysis results for a 1T-CT specimen based on data given in Ref. 81.

$T = -75°C \quad B = 25.4$ mm
$E = 207$ GPa
$\sigma_Y = 483$ MPa

$$\varepsilon_z = \frac{\partial w}{\partial z} \qquad \beta = \frac{EJ}{\sigma_Y^2 B}$$

P (kN)	J (kJ/m^2)		$\varepsilon_z @ z = 0$ (%)	β
29	15.7	-	0.059	0.55
35	23.7	-	0.081	0.83
50	67.3	-	0.191	2.36

stress peak is being supplied from the through-thickness direction. This implies that slip lines have extended from the mid-plane to the free side surfaces without curvature, thus allows plastic tensile strain to develop near the crack tip without stress elevation except for strain hardening.

Some qualitative substantiation of the hypothesis just described can be found in the results of an additional large-strain, elastic-plastic analysis for an axial, external semielliptical surface crack in the cylinder of a pressure vessel, also performed by Brocks [100]. The values of crack-opening stress at a fixed small distance from the crack front, as a function of the parametric angle of the semiellipse, measured from the deepest point, slowly approach a maximum as the angle increases, then drop suddenly, shortly after the tangential contraction strain passes - 0.6% on the way to becoming more negative. Thus, it appears that the ease with which negative plastic strain can occur near the crack tip, in the plane of the crack, and the curvature of the slip lines associated with the directions of its occurrence, are prime determinants of constraint.

CONCLUSIONS

This paper began with a brief philosophical and historical overview of applied fracture mechanics, particularly as it pertains to the safety of pressure vessels. It then progressed to a more-or-less chronological panorama of experimental and analytical results pertaining to the important subject of constraint, a fundamental aspect of fracture mechanics in which Jerry Swedlow had a keen interest and to which he made valuable contributions. A central theme of this paper has been that, in accordance with the scientific method, the search for patterns is constant and vital. This theme is well illustrated historically by the development of small, single-specimen, fracture toughness testing techniques. It is also illustrated here by the development, based on two different published large-strain, elastic-plastic, three-dimensional finite-element analyses, of a hypothesis concerning three-dimensional loss of constraint. Specifically, it appears that, at least in standard compact specimens, when a generalization of Irwin's thickness-normalized plastic-zone parameter, β, reaches a value close to 2π, the through-thickness contraction strain at the apex of the near-tip logarithmic-spiral slip-line region becomes the dominant negative strain

accommodating crack opening. Because slip lines passing from the midplane to the stress-free side surfaces do not have to curve, once these slip lines are established, stresses near the crack tip are only elevated by strain hardening and constraint becomes significantly relaxed. This hypothesis, based on published three-dimensional elastic-plastic analyses, provides a potentially valuable means for gaining additional insight into constraint effects on fracture toughness by considering the roles played by the plastic strains as well as the stresses that develop near a crack tip.

ACKNOWLEDGMENT

This research was sponsored by the Office of Nuclear Regulatory Research, U.S. Nuclear Regulatory Commission under Interagency Agreement 1886-8011-9B with the U.S. Department of Energy under Contract DE-AC05-84OR21400 with Martin Marietta Energy Systems, Inc. The submitted manuscript has been authored by a contractor of the U.S. Government under Contract No. DE-AC05-84OR21400. Accordingly, the U.S. Government retains a non-exclusive, royalty-free license to publish or reproduce the published form of this contribution, or allow others to do so, for U.S. Government purposes.

REFERENCES

1. Irwin, G. R. and Kies, J. A., "Critical Energy Rate Analysis of Fracture Strength," *Welding Journal*, Research Supplement, April 1954, pp. 193-S - 198-S.

2. Irwin, G. R., "Analysis of Stresses and Strains Near the End of a Crack Traversing a Plate," *Journal of Applied Mechanics*, September 1957, pp. 361-364.

3. Pellini, W. S. and Puzak, P. P., "Fracture Analysis Diagram Procedures for the Fracture-Safe Engineering Design of Steel Structures," *Welding Research Council Bulletin No. 88*, May 1963.

4. Irwin, G. R., "Crack-Toughness Testing of Strain-Rate Sensitive Materials," *Journal of Engineering for Power*, ASME, October 1964, pp. 444-450.

5. Brown, W. F. (ed.), *Review of Developments in Plane Strain Fracture Toughness Testing*, ASTM STP 463, American Society for Testing and Materials, Philadelphia, Pennsylvania, 1970.

6. Loss, F. J., "Dynamic Tear Test Investigations of the Fracture Toughness of Thick-Section Steel," NRL Report 7056 (HSSTP-TR-7), Naval Research Laboratory, Washington, D.C., May 14, 1970.

7. Shabbits, W. O., Pryle, W. H., and Wessel, E. T., "Heavy Section Fracture Toughness Properties of A533 Grade B, Class 1 Steel Plate and Submerged Arc Weldment," WCAP-7414 (HSSTP-TR-6), Westinghouse Electric Corporation, Pittsburgh, Pennsylvania, December 1969.

8. Shabbits, W. O., "Dynamic Fracture Toughness Properties of Heavy Section A533 Grade B, Class 1 Steel Plate," Westinghouse Electric Corporation, Pittsburgh, Pennsylvania, December 1970.

9. Crosley, P. B. and Ripling, E. J., "Plane Strain Crack Arrest Characterization of Steels," *Journal of Pressure Vessel Technology*, ASME, November 1975, pp. 291-298.

10. *ASME Boiler and Pressure Vessel Code*, Section XI, Rules for Inservice Inspection of Nuclear Power Plant Components, Appendix A, Evaluation of Flaw Indications, July 1, 1974.

11. Merkle, J. G. "A Summary of the Low Upper Shelf Toughness Safety Margin Issue," *Pressure Vessel Integrity - 1991*, PVP-Vol. 213 (MPC-Vol. 32), ASME, June 1991, pp. 89-98.

12. Sorem, W. A., Rolfe, S. T., and Dodds, R. H., Jr., "The Effects of Crack Depth on Elastic-Plastic CTOD Fracture Toughness," *WRC Bulletin 351*, Welding Research Council, New York, New York, February 1990, pp. 12-23.

13. Theiss, T. J. and Bryson, J. W., "Influence of Crack Depth on the Fracture Toughness of Reactor Pressure Vessel Steel," *Constraint Effects in Fracture*, ASTM STP 1171, American Society for Testing and Materials, Philadelphia, Pennsylvania, 1993, pp. 104-119.

14. Shih, C. F. and Zia, L., "Modeling Crack Growth Resistance Using Computational Cells with Microstructurally-Based Length Scales," *Constraint Effects in Fracture: Theory and Applications*, ASTM STP 1244, American Society for Testing and Materials, Phildelphia, Pennsylvania (in press).

15. Wallin, K., "Statistical Aspects of Constraint with Emphasis on Testing and Analysis of Laboratory Specimens in the Transition Region," *Constraint Effects in Fracture*, ASTM STP 1171, American Society for Testing and Materials, Philadelphia, Pennsylvania, 1993, pp. 264-288.

16. Wells, A. A., "Notched Bar Tests, Fracture Mechanics, and the Brittle Strengths of Welded Structures," *British Welding Journal*, January 1965, pp. 2-13.

17. Witt, F. J. and Mager, T. R., "Fracture Toughness K_{Icd} Values at Temperatures up to 550°F for ASTM A533, Grade B, Class 1 Steel," *Nuclear Engineering and Design*, Vol. 17, 1971, pp. 91-102.

18. Rice, J. R., "A Path Independent Integral and the Approximate Analysis of Strain Concentration by Notches and Cracks," *Journal of Applied Mechanics*, ASME, June 1968, pp. 379-386.

19. Rice, J. R., "Mathematical Analysis in the Mechanics of Fracture," Chapter 3 in Vol. 2 of *Fracture, an Advanced Treatise*, H. Liebowitz, ed., Academic Press, 1968.

20. Begley, J. A. and Landes, J. D., "The J-Integral as a Fracture Criterion," *Fracture Toughness*, Part II, ASTM STP 514, American Society for Testing and Materials, Philadelphia, Pennsylvania, 1972, pp. 1-23.

21. Landes, J. D. and Begley, J. A., "The Effect of Specimen Geometry on J_{Ic}," *Fracture Toughness*, Part II, ASTM STP 514, American Society for Testing and Materials, Philadelphia, Pennsylvania, 1972, pp. 24-39.

22. Paris, P. C., "Fracture Mechanics in the Elastic-Plastic Regime," *Flaw Growth and Fracture*, ASTM STP 631, American Society for Testing and Materials, Philadelphia, Pennsylvania, 1977, pp. 3-27.

23. Rice, J. R., Paris, P. C., and Merkle, J. G., "Some Further Results of J-Integral Analysis and Estimates," *Progress in Flaw Growth and Fracture Toughness Testing*, ASTM STP 536, American Society for Testing and Materials, Philadelphia, Pennsylvania, 1973, pp. 231-245.

24. Merkle, J. G. and Corten, H. T., "A. J-Integral Analysis for the Compact Specimen, Considering Axial Force as well as Bending Effects," *Journal of Pressure Vessel Technology*, Vol. 96, No. 4, ASME, November 1974, pp. 286-292.

25. Ernst, H. A., Paris, P. C., and Landes, J. D., "Estimations on J-Integral and Tearing Modulus T from a Single Specimen Test Record," *Fracture Mechanics, Thirteenth Conference*, ASTM STP 743, American Society for Testing and Materials, Philadelphia, Pennsylvania, 1981, pp. 476-502.

26. Randall, P. N. and Merkle, J. G., "Gross Strain Crack Tolerance of Steels," *Nuclear Engineering and Design*, Vol. 17, 1971, pp. 46-63.

27. Randall, P. N. and Merkle, J. G., "Effects of Strain Gradients on the Gross Strain Crack Tolerance of A533-B Steel," *Progress in Flaw Growth and Fracture Toughness Testing*, ASTM STP 536, American Society for Testing and Materials, Philadelphia, Pennsylvania, 1973, pp. 404-420.

28. Merkle, J. G., "Development of the Tangent Modulus Method of Elastic-Plastic Fracture Analysis," *Fracture Mechanics Applications: Implications of Detected Flaws*, IAEA-189, International Atomic Energy Agency, Vienna, 1976, pp. 407-460.

29. Grigory, S. C., "Testing the Six-Inch Thick Flawed Tensile Specimen for the Heavy Section Steel Technology Program," *Nuclear Engineering and Design*, Vol. 17, 1971, pp. 161-169.

30. Hall, W. J., Kihara, H., Soete, W., and Wells, A. A., *Brittle Fracture of Welded Plate*, Prentice-Hall, Inc., Englewood Cliffs, New Jersey, 1967 (see also Prof. Mylonas' written discussion of Ref. 40 cited later in this paper).

31. Loechel, L. W., "The Effect of Testing Variables on the Transition Temperature in Steel," MCR 69-189 (HSSTP-TR-2), Martin Marietta Corporation, Denver, Colorado, November 20, 1969.

32. Merkle, J. G., Koostra, L. F., and Derby, R. W., "Interpretations of the Drop Weight Test in Terms of Strain Tolerance (Gross Strain) and Fracture Mechanics," ORNL-TM-3247, Oak Ridge National Laboratory, Oak Ridge, Tennessee, June 1971.

33. Whitman, G. D., "Historical Summary of the Heavy-Section Steel Technology Program and Some Related Activities in Light-Water Reactor Pressure Vessel Safety Research," NUREG/CR-4489, Oak Ridge National Laboratory, Oak Ridge, Tennessee, March 1986.

34. Merkle, J. G., Whitman, G. D., and Bryan, R. H., "Relation of Intermediate-Sized Pressure-Vessel Tests to LWR Safety," *Nuclear Safety*, Vol. 17, No. 4, July-August 1976, pp. 447-463.

35. Cheverton, R. D., Iskander, S. K., and Ball, D. G., "Review of Pressurized-Water-Reactor-Related Thermal Shock Studies," *Fracture Mechanics: Nineteenth Symposium*, ASTM STP 969, American society for Testing and Materials, Philadelphia, Pennsylvania, 1988, pp. 752-766.

36. Theiss, T. J., Shum, D. K., and Rolfe, S. T., "Experimental and Analytical Investigation of the Shallow-Flaw Effect in Reactor Pressure Vessels," NUREG/CR-5886, Oak Ridge National Laboratory, Oak Ridge, Tennessee, July 1992.

37. Bryan, R. H., Merkle, J. G., Nanstad, R. K., and Robinson, G. C., "Pressurized Thermal Shock Experiments with Thick Vessels," *Fracture Mechanics: Nineteenth Symposium*, ASTM STP 969, American Society for Testing and Materials, Philadelphia, Pennsylvania, 1988, pp. 767-783.

38. Bryan, R. H. et al., "Performance of Low-Upper-Shelf Material Under Pressurized-Thermal-Shock Loading," *Nuclear Engineering and Design*, Vol. 115, 1989, pp. 359-367.

39. Irwin, G. R., Kies, J. A., and Smith, H. L., "Fracture Strengths Relative to Onset and Arrest of Crack Propagation," *ASTM Transactions*, Vol. 58, American Society for Testing and Materials, Philadelphia, Pennsylvania, 1958, pp. 640-660.

40. Irwin, G. R., "Fracture Mechanics," *Structural Mechanics*, Proceedings of the First Symposium on Naval Structural Mechanics, Pergamon Press, 1960, pp. 557-594.

41. Irwin, G. R., "Dimensional and Geometric Aspects of Fracture," *Fracture of Engineering Materials*, American Society for Metals, 1964, pp. 211-230.

42. Irwin, G. R., "Fracture Mode Transition for a Crack Traversing a Plate," *Journal of Basic Engineering*, Vol. 82, No. 2, ASME, June 1960, pp. 417-425.

43. Irwin, G. R., "Plastic Zone Near a Crack and Fracture Toughness," *Proceedings of the Seventh Sagamore Ordnance Materials Research Conference*, Syracuse University Research Institute, 1960, pp. IV-63 to IV-78.

44. Irwin, G. R., "Relation of Crack Toughness Measurements to Practical Applications," *Welding Research Supplement*, Vol. 41, No. 11, November 1962, pp. 519s-528s.

45. Irwin, G. R., "Structural Aspects of Brittle Fracture," *Applied Materials Research*, Vol. 3, No. 2, April 1964, pp. 65-81.

46. Wessel, E. T., "Relation of Laboratory Determinations of Fracture Toughness with the Performance of Large Steel Pressure Vessels," *Welding Journal, Research Supplement*, Vol. 43, No. 9, September 1964, pp. 415s-424s.

47. Lubahn, J. D., "A Review of Engineering Approaches to Brittle Fracture Design," (no document number) Colorado School of Mines, Golden, Colorado, 1961.

48. Weiss, V., "Material Ductility and Fracture Toughness of Metals," *Mechanical Behavior of Materials*, Vol. 1, The Society of Materials Science, Japan, 1972, pp. 458-474.

49. Lequear, H. A. and Lubahn, J. D., "Root Conditions in a V-Notch Charpy Impact Specimen," *Welding Journal Research Supplement*, December 1954, pp. 585-s - 588-s.

50. Clausing, D. P., "Effect of Plastic Strain State on Ductility and Toughness," *International Journal of Fracture Mechanics*, Vol. 6, No. 1, March 1970, pp. 71-85.

51. Barsom, J. M., "Relationship Between Plane Strain Ductility and K_{Ic}" *Journal of Engineering for Industry*, Vol. 93, No. 4, ASME, November 1971, pp. 1209-1215.

52. Merkle, J. G., "An Elastic-Plastic Thick-Walled Hollow Cylinder Analogy for Analyzing the Strains in the Plastic Zone Just Ahead of a Notch Tip," ORNL-TM-4071, Oak Ridge National Laboratory, Oak Ridge, Tennessee, January 1973.

53. Malkin, J. and Tetelman, A. S., "Relation Between K_{Ic} and Microscopic Strength for Low Alloy Steels," Report No. 69-58, Materials Department, University of California, Los Angeles, California, August 1969.

54. Neuber, H., "Theory of Stress Concentration for Shear-Strained Prismatical Bodies with Arbitrary Nonlinear Stress-Strain Law," *Journal of Applied Mechanics*, ASME, December 1961, pp. 544-550.

55. Harrison, J. D., "A Comparison Between Four Elasto-Plastic Fracture Mechanics Parameters," R/RB/E64/75, The Welding Institute, Abington Hall, Cambridge, England, January 1975.

56. Dawes, M. G., "Elastic-Plastic Fracture Toughness Based on the COD and J-Contour Integral Concepts," *Elastic-Plastic Fracture*, ASTM STP 668, American Society for Testing and Materials, Philadelphia, Pennsylvania, 1979, pp. 307-333.

57. Wellman, G. W., Rolfe, S. T., and Dodds, R. H., "Three-Dimensional Elastic-Plastic Finite Element Analysis of Three-Point Bend Specimens," *WRC Bulletin 299*, Welding Research Council, New York, New York, November 1984, pp. 15-25.

58. Wilson, A. D. and Donald, J. K., "Evaluating Steel Toughness Using Various Elastic-Plastic Fracture Toughness Parameters," *Nonlinear Fracture Mechanics: Vol. II - Elastic-Plastic Fracture*, ASTM STP 995, American Society for Testing and Materials, Philadelphia, Pennsylvania, 1989, pp. 144-168.

59. Sorem, W. A., Dodds, R. H., Jr., and Rolfe, S. T., "A Comparison of the J-Integral and CTOD Parameters for Short Crack Specimen Testing," *WRC Bulletin 341*, Welding Research Council, New York, New York, February 1990, pp. 24-34.

60. Landes, J. D., McCabe, D. E., and Ernst, H. A., "Geometry Effects on the R-Curve," *Nonlinear Fracture Mechanics: Vol. II - Elastic-Plastic Fracture*, ASTM STP 995, American Society for Testing and Materials, Philadelphia, Pennsylvania, 1989, pp. 123-143.

61. McMeeking, R. M. and Parks, D. M., "On Criteria for J-Dominance of Crack-Tip Fields in Large-Scale Yielding," *Elastic-Plastic Fracture*, ASTM STP 668, American Society for Testing and Materials, Philadelphia, Pennsylvania, 1979, pp. 175-194.

62. Sorem, W. A., Dodds, R. H., Jr., and Rolfe, S. T., "An Analytical Comparison of Short Crack and Deep Crack CTOD Fracture Specimens of an A36 Steel," *WRC Bulletin 351*, Welding Research Council, New York, New York, February 1990, pp. 1-11.

63. Smith, C. W., Jolles, M., and Peters, W. H., "Stress Intensities in Flawed Pressure Vessels," *Proceedings of the Third International Conference on Pressure Vessel Technology, Part II - Materials and Fabrication*, Tokyo, ASME, April 1977, pp. 535-543.

64. Bilby, B. A., Cardew, G. E., Goldthorpe, M. R., and Howard, D. C., "A Finite Element Investigation of the Effect of Specimen Geometry on the Fields of Stress and Strain at the Tips of Stationary Cracks," *Size Effects in Fracture*, The Institution of Mechanical Engineers, London, 1986, pp. 37-56.

65. Hancock, J. W., Reuter, W. G., and Parks, D. M., "Constraint and Toughness Parameterized by T," *Constraint Effects in Fracture*, ASTM STP 1171, American Society for Testing and Materials, Philadelphia, Pennsylvania, 1993, pp. 21-40.

66. Shih, C. F., O'Dowd, N. P., and Kirk, M. T., "A Framework for Quantifying Crack Tip Constraint," *Constraint Effects in Fracture*, ASTM STP 1171, American Society for Testing and Materials, Philadelphia, Pennsylvania, 1993, pp. 2-20.

67. Shum, D. K. M. and Merkle, J. G., "Crack Initiation Under Generalized Plane-Strain Conditions," *Fracture Mechanics: Twenty-Third Symposium*, ASTM STP 1189, American Society for Testing and Materials, Philadelphia, Pennsylvania, 1993, pp. 37-54.

68. Anderson, T. L. and Dodds, R. H., Jr., "Specimen Size Requirements for Fracture Toughness Testing in the Transition Region," *Journal of Testing and Evaluation*, Vol. 19, No. 2, JTEVA, March 1991, pp. 123-134.

69. Anderson, T. L., Vanaparthy, N. M. R., and Dodds, R. H., Jr., "Predictions of Specimen Size Dependence on Fracture Toughness for Cleavage and Ductile Tearing," *Constraint Effects in Fracture*, ASTM STP 1171, American Society for Testing and Materials, Philadelphia, Pennsylvania, 1993, pp. 473-491.

70. Dodds, R. H., Jr., Shih, C. F., and Anderson, T. L., "Continuum and Micromechanics Treatment of Constraint in Fracture," UILU-ENG-92-2014, Department of Civil Engineering, University of Illinois, Urbana, Illinois, November 1992.

71. Yang, S., Chao, Y. J., and Sutton, M. A., "Complete Theoretical Analysis for Higher Order Asymptotic Terms and the HRR Zone at a Crack Tip for Mode I and Mode II Loading of a Hardening Material," *Acta Mechanica*, Vol. 98, 1993, pp. 79-98.

72. Chao, Y. J., Yang, S., and Sutton, M. A., "On the Fracture of Solids Characterized by One or Two Parameters: Theory and Practice," *Journal of the Mechanics and Physics of Solids*, Vol. 42, No. 4, 1994, pp. 629-647.

73. Yang, S., Chao, Y. J., and Sutton, M. A., "Higher Order Asymptotic Crack Tip Fields in a Power-Law Hardening Material," *Engineering Fracture Mechanics*, Vol. 45, 1993, pp. 1-20.

74. Chao, Y. J., and Ji, W., "Cleavage Fracture Quantified by J and A_2," *Constraint Effects in Fracture: Theory and Application*," ASTM STP 1244, American Society for Testing and Materials, Philadelphia, 1995.

75. Chao, Y. J., "On a Single Parameter Controlled Fracture of Solids Under Plane Stress Conditions," *International Journal of Fracture*, Vol. 62, 1993, pp. R7-R10.

76. Xia, L., Wang, T. C., and Shih, C. F., "Higher-Order Analysis of Crack-Tip Fields in Elastic Power-Law Hardening Materials," *Journal of the Mechanics and Physics of Solids*, Vol. 41, 1993, pp. 665-687.

77. Hutchinson, J. W., "Singular Behavior at the End of a Tensile Crack in a Hardening Material," *Journal of the Mechanics and Physics of Solids*, Vol. 16, 1968, pp. 13-31.

78. Rice, J. R. and Rosengren, G. F., "Plane Strain Deformation Near a Crack Tip in a Power-Law Hardening Material," *Journal of the Mechanics and Physics of Solids*, Vol. 16, 1968, pp. 1-12.

79. Hutchinson, J. W., "Plastic Stress and Strain Fields at a Crack Tip," *Journal of the Mechanics and Physics of Solids*, Vol. 16, 1968, pp. 337-347.

80. Swedlow, J. L., "The Thickness Effect and Plastic Flow in Cracked Plates," ARL 65-216, Aerospace Research Laboratories, Office of Aerospace Research, United States Air Force, Wright-Patterson Air Force Base, Ohio, October 1965.

81. Bass, B. R., Shum, D. K., and Keeney-Walker, J., "Constraint Effects on Fracture Toughness for Circumferentially Oriented Cracks in Reactor Pressure Vessels," NUREG/CR-6008, Oak Ridge National Laboratory, Oak Ridge, Tennessee, August 1992.

82. Pennell, W. E., Bass, B. R., Bryson, J. W., McAfee, W. J., Theiss, T. J., and Rao, M. C., "Biaxial Loading and Shallow-Flaw Effects on Crack-Tip Constraint and Fracture Toughness," *Changing Priorities of Codes and Standards*, PVP-Vol. 286, ASME, 1994, pp. 103-114.

83. Milne, I. and Curry, D. A., "Ductile Crack Growth Analysis Within the Ductile-Brittle Transition Regime: Predicting the Permissible Extent of Ductile Crack Growth," RD/L/2209N81, Central Electricity Research Laboratories, Central Electricity Generating Board, United Kingdom, March 1982.

84. Varias, A. G. and Shih, C. F., "Quasi-Static Crack Advance Under a Range of Constraints: Steady-State Fields Based on a Characteristic Length" *Journal of the Mechanics and Physics of Solids*, Vol. 41, No. 5, 1993, pp. 835-861.

85. Tang, M., Dodds, R. H., Jr., and Anderson, T. L., "Effects of Ductile Crack Growth on Constraint Models for Cleavage Fracture," UILU-ENG-94-2001, Department of Civil Engineering, University of Illinois, Urbana, Illinois, January 1994.

86. Averbach, B. L., "Physical Metallurgy and Mechanical Properties of Materials: Brittle Fracture," Paper No. 2686, *Journal of the Engineering Mechanics Division*, ASCE, Vol. 86, No. EM6, December 1960, pp. 29-43.

87. Averbach, B. L., "Some Physical Aspects of Fracture," Chapter 7 in *Fracture, An Advanced Treatise*, Vol. 1, Academic Press, New York, 1968.

88. Hahn, G. T., "The Influence of Microstructure on Brittle Fracture Toughness," *Metallurgical Transactions A*, Vol. 15A, June 1984, pp. 947-959.

89. Irwin, G. R. and Zhang, X. J., "Cleavage Behaviors in Nuclear Vessel Steels," *Pressure Vessel Integrity*, PVP-Vol. 250, ASME, 1993, pp. 11-17.

90. Irwin, G. R., Zhang, X. J., and Schwartz, C. W., "Small Scale Nonuniformities Related to Cleavage Initiation and their Implications for Constraint Modeling," ORNL/NRC/LTR-94/18, Oak Ridge National Laboratory, Oak Ridge, Tennessee, August 1994.

91. Swedlow, J. L. and Ritter, M. A., "Toward Assessing the Effects of Crack Front Curvature (CFC)," *Stress Analysis and Growth of Cracks*, Part I, ASTM STP 513, American Society for Testing and Materials, Philadelphia, Pennsylvania, 1971, pp. 79-89.

92. Malik, S. N. and Fu, L. S., "Elasto-Plastic Analysis for a Finite Thickness Rectangular Plate Containing a Through-Thickness Central Crack," *International Journal of Fracture*, Vol. 18, No. 1, 1982.pp. 45-63.

93. Merkle, J. G., "Constraint and Strain Rate Effects in Fracture Toughness Testing," *Proceedings of the Fifteenth Water Reactor Safety Information Meeting*, NUREG/CP-0091, U.S. Nuclear Regulatory Commission, Washington, D.C., February 1988, pp. 5-15.

94. Newman, J. C., Jr., Crews, J. H., Bigelow, C. A., and Dawicke, D. S., "Variations of a Global Constraint Factor in Cracked Bodies Under Tension and Bending Loads," NASA Technical Memorandum 109119, National Aeronautics and Space Administration, Langley Reaearch Center, Hampton, Virginia, May 1994.

95. Shum, D. K. M., "Effects of 3-D Transverse Constraint on the Evolution of In-Plane Q-Stress," *Fracture Mechanics*, Vol. 26, ASTM STP 1256, American Society for Testing and Materials, Philadelphia, Pennsylvania, (in press).

96. Sommer, E. and Aurich, D., "On the Effect of Constraint on Ductile Fracture," *Defect Assessment in Components*, ESIS/EGF 9 Mechanical Engineering Publications, London, 1991, pp. 141-174.

97. Brocks, W., Künecke, G., Noack, H. D., and Veith, H., "On the Transferability of Fracture Mechanics Parametes from Specimens to Structures Using FEM," *Nuclear Engineering and Design*, Vol. 112, 1989, pp. 1-14.

98. Merkle, J. G., "An Examination of the Size Effects and Data Scatter Observed in Small-Specimen Cleavage Fracture Toughness Testing," NUREG/CR-3672, Oak Ridge National Laboratory, Oak Ridge, Tennesssee, April 1984.

99. McCabe, D. E., "A Comparison of Weibull and b_{Ic} Analyses of Transition Range Data," *Fracture Mechanics: Twenty-Third Symposium*, ASTM STP 1189, American Society for Testing and Materials, Philadelphia, Pennsylvania, 1993, pp. 80-94.

100. Brocks, W. and Künecke, G., "Elastic-Plastic Fracture Mechanics Analysis of a Pressure Vessel with an Axial Outer Surface Flaw (Part 2)," ORNL/TR-89/48 (translation of BAM Research Report No. 137, Berlin, Germany, June 1989), Oak Ridge National Laboratory, Oak Ridge, Tennessee, 1989.